Contrasting Levels of Molecular Evolution on the Mouse X Chromosome

Erica L. Larson,* Dan Vanderpool,* Sara Keeble,*,† Meng Zhou,† Brice A. J. Sarver,* Andrew D. Smith,† Matthew D. Dean,† and Jeffrey M. Good*,1

*Division of Biological Sciences, University of Montana, Missoula, Montana 59812 and †Molecular and Computational Biology, University of Southern California, Los Angeles, California 90089

ABSTRACT The mammalian X chromosome has unusual evolutionary dynamics compared to autosomes. Faster-X evolution of spermatogenic protein-coding genes is known to be most pronounced for genes expressed late in spermatogenesis, but it is unclear if these patterns extend to other forms of molecular divergence. We tested for faster-X evolution in mice spanning three different forms of molecular evolution—divergence in protein sequence, gene expression, and DNA methylation—across different developmental stages of spermatogenesis. We used FACS to isolate individual cell populations and then generated cell-specific transcriptome profiles across different stages of spermatogenesis in two subspecies of house mice (*Mus musculus*), thereby overcoming a fundamental limitation of previous studies on whole tissues. We found faster-X protein evolution at all stages of spermatogenesis and faster-late protein evolution for both X-linked and autosomal genes. In contrast, there was less expression divergence late in spermatogenesis (slower late) on the X chromosome and for autosomal genes expressed primarily in testis (testis-biased). We argue that slower-late expression divergence reflects strong regulatory constraints imposed during this critical stage of sperm development and that these constraints are particularly acute on the tightly regulated sex chromosomes. We also found slower-X DNA methylation divergence based on genome-wide bisulfite sequencing of sperm from two species of mice (*M. musculus* and *M. spretus*), although it is unclear whether slower-X DNA methylation reflects development constraints in sperm or other X-linked phenomena. Our study clarifies key differences in patterns of regulatory and protein evolution across spermatogenesis that are likely to have important consequences for mammalian sex chromosome evolution, male fertility, and speciation.

KEYWORDS faster X evolution; gene expression; DNA methylation; fluorescence-activated cell sorting; postmeiotic sex chromosome repression (PSCR)

THE X chromosome plays a disproportionately large role in adaptation and speciation (Bachtrog *et al.* 2011; Ellegren 2011; Charlesworth 2013), but the underlying molecular and evolutionary drivers of these patterns remain unclear. On one hand, the X chromosome often shows strong signatures of evolutionary constraint. For example, the evolution of dosage compensation via epigenetic X-chromosome inactivation (XCI) in females (Lyon 1961, 1962) imposes regulatory constraints that select for strong conservation of X-linked gene content in placental mammals (Ohno 1967; Kohn *et al.* 2004). On the other hand, these inherent constraints are punctuated by strong specialization in X-linked gene content (Emerson *et al.* 2004; Mueller *et al.* 2008, 2013; Potrzebowski *et al.* 2008; Zhang *et al.* 2010; Sin *et al.* 2012) and numerous examples of rapid X-linked evolution (Torgerson and Singh 2003, 2006; Baines and Harr 2007; Kousathanas *et al.* 2014; Nam *et al.* 2015).

The X chromosome is predicted to evolve faster than the autosomes if beneficial mutations are on average recessive because selection will act more efficiently on X-linked mutations exposed in hemizygous males (Charlesworth *et al.* 1987). Under this model, faster-X evolution should be most intense for male-specific genes (Rice 1984; Vicoso and Charlesworth 2009). Indeed, the strongest evidence for faster-X evolution comes from patterns of protein-coding evolution during spermatogenesis (Torgerson and Singh 2006; Baines *et al.* 2008; Grath and Parsch 2012; Sin *et al.* 2012; Kousathanas

doi: 10.1534/genetics.116.186825
Manuscript received February 9, 2016; accepted for publication June 8, 2016; published Early Online June 14, 2016.
Supplemental material is available online at www.genetics.org/lookup/suppl/doi:10.1534/genetics.116.186825/-/DC1.
[1]Corresponding author: Division of Biological Sciences, University of Montana, 32 Campus Drive, HS 104, Missoula, MT 59812. E-mail: jeffrey.good@mso.umt.edu

et al. 2014). Molecular evolution on the X chromosome may also differ from the autosomes due to a smaller effective population size (*i.e.*, 3/4 autosomal N_e assuming equal sex ratios) (Vicoso and Charlesworth 2009; Mank *et al.* 2010) or sex-linked differences in mutation rates (μ) (Miyata *et al.* 1987; Begun and Whitley 2000; Ellegren 2007). Differences in N_e and μ aside, the theoretical expectations for faster-X evolution should extend to other functional aspects of DNA sequence evolution. Gene regulation is usually measured through various biochemical phenotypes (*e.g.*, transcript abundances, methylation patterns) that may not directly reflect linked sequence evolution, yet accelerated divergence of X-linked gene expression levels has been reported in fruit flies (Kayserili *et al.* 2012; Meisel *et al.* 2012a; Coolon *et al.* 2015; Llopart 2015), birds (Dean *et al.* 2015), and mammals (Khaitovich *et al.* 2005a; Zhang *et al.* 2010; Brawand *et al.* 2011). The evolution of other regulatory phenotypes has not been widely considered and the extent to which different forms of molecular evolution show similar patterns of X-linked evolution remains to be seen.

A critical evaluation of molecular evolution in the male germ line depends on a few important details of spermatogenesis. Spermatogenesis is defined by progressive gene specialization, with postmeiotic genes tending to be more narrowly expressed and functionally specific (Eddy 2002; Schultz *et al.* 2003; Good and Nachman 2005). Expression breadth and specialization influence rates of protein-coding evolution (Liao *et al.* 2006; Ellegren and Parsch 2007; Meisel *et al.* 2012b) and genes expressed later in spermatogenesis show more rapid protein-coding evolution (Good and Nachman 2005; Sin *et al.* 2012). Yet there remain relatively few examples where patterns of divergence have been evaluated across different stages of spermatogenesis (Good and Nachman 2005; Kousathanas *et al.* 2014), and how different forms of molecular evolution change in this developmental context is largely unknown. The sex chromosomes are also silenced during male meiosis through meiotic sex chromosome inactivation (MSCI) (Turner 2007). This period of inactivation results in strong selection against X-linked genes that need to be expressed during meiosis, while genes expressed prior to MSCI are enriched on the X chromosome (Wang *et al.* 2001; Khil *et al.* 2004). Gene expression remains transcriptionally repressed in postmeiotic stages of spermatogenesis [postmeiotic sex chromosome repression (PSCR)], although several X-linked genes overcome PSCR and are highly expressed in round spermatids (Namekawa *et al.* 2006; Mueller *et al.* 2008; Sin *et al.* 2012). In general, X-linked genes expressed during PSCR tend to be more specialized with narrower expression profiles and show more rapid protein evolution relative to coexpressed autosomal genes (Sin *et al.* 2012; Kousathanas *et al.* 2014).

While the context and timing of expression during spermatogenesis play crucial roles in the interpretation of faster-X protein evolution, most comparative expression studies have focused on whole tissues. This experimental approach implicitly assumes that differential gene expression between species is not simply an artifact of differences in cell composition. Yet spermatogenesis is usually asynchronous and overlapping in mature testis, leading to age-dependent heterogeneity in the abundances of germ cell populations through time. Testis cellular composition (*i.e.*, testis histology) may also evolve rapidly when selection from sperm competition results in allometric shifts toward more sperm-producing seminiferous tubules (Firman *et al.* 2015). Such technical issues confound patterns of gene expression measured from whole testis (Good *et al.* 2010), especially when combined with differences in stages of maturity, levels of fertility, or comparisons between species. For example, testis expression patterns in primates cluster more strongly with mating system than evolutionary relatedness (Brawand *et al.* 2011; Saglican *et al.* 2014), indicating that testis transcriptomes are strongly influenced by convergent shifts in cellular composition associated with different reproductive strategies. When combined with considerable variation in relative enrichment for or against X linkage across different stages of spermatogenesis (Khil *et al.* 2004), it is apparent that a rigorous examination of faster-X gene expression evolution requires a cell- or stage-specific approach.

Here we report two experiments designed to evaluate three different forms of molecular evolution across spermatogenesis in mice. First, we used fluorescence-activated cell sorting (FACS) (Getun *et al.* 2011) and RNA sequencing (RNA-seq) (Wang *et al.* 2009) to generate transcriptomes from mitotic, meiotic, and postmeiotic spermatogenic cells in two subspecies of house mice (*Mus musculus musculus* and *M. m. domesticus*). We quantified genome-wide patterns of protein-coding and expression divergence across key developmental stages of spermatogenesis and tested for faster-X molecular evolution. Second, we performed whole genome bisulfite sequencing (BS-seq) (Frommer *et al.* 1992) to quantify patterns of DNA methylation divergence between sperm from house mice (*M. m. musculus*) and the closely related Algerian mouse (*M. spretus*). This second experiment allowed us to quantify the evolution of a key regulatory phenotype on and off the X chromosome for the first time in mice. Collectively, these experiments allow us to quantify different molecular evolutionary patterns in light of specific stages of sperm development.

Materials and Methods

Experimental design and choice of mouse strains

Information on protein-coding evolution between *M. m. musculus*, *M. m. domesticus*, and *M. spretus* is accessible using published genomic resources (Keane *et al.* 2011). However, the technical demands and experimental resources necessary to generate novel cell-specific transcriptome and DNA methylation data across spermatogenesis in all three lineages are reasonably beyond the scope of a single study. Therefore, we used a nested subset of evolutionary contrasts to optimize our power to quantify gene expression and methylation divergence. Divergence in gene expression levels accumulates relatively quickly (Lemos

et al. 2004) and so we focused our FACS-based partitioning of gene expression across spermatogenesis on two subspecies of house mice (*M. m. domesticus* and *M. m. musculus*). We used four wild-derived inbred strains (purchased from The Jackson Laboratory, Bar Harbor, ME) to generate interstrain F_1's for each subspecies (*M. m. musculus*: CZECHII/EiJ females × PWK/PhJ males; *M. m. domesticus*: WSB/EiJ females × LEWES/EiJ males). This crossing design reduces the impacts of inbreeding depression on basic reproductive phenotypes and follows previous studies on these mice (Good *et al.* 2008, 2010; Campbell *et al.* 2013). Less in known about the evolutionary tempo of DNA methylation divergence, but patterns of methylation can be highly conserved between species (Molaro *et al.* 2011). Therefore, we focused our analysis of sperm DNA methylation on contrasts between *M. spretus* and *M. m. musculus* represented by four partially inbred strains of *M. spretus* (SFM and STF) and *M. m. musculus* (MPB and MBS) acquired from François Bonhomme (University of Montpellier, Montpellier, France).

Gene expression and DNA methylation experiments were initiated independently at the University of Montana (UM) (expression) and the University of Southern California (USC) (methylation) using different strains of mice. To confirm the expected evolutionary relationships among the mouse strains used in this study, we estimated a phylogeny using published whole genome data for WSB/EiJ and SPRET/EiJ (Keane *et al.* 2011) and new whole exome data from all other strains. Whole exomes were enriched for Illumina sequencing using an in-solution NimbleGen SeqCap EZ Mouse (Roche) exome design targeting 54.3 Mb of exonic regions in the mouse genome (Fairfield *et al.* 2011). This in-solution platform performs well when used across different species of *Mus* with minimal biases in capture efficiency and sensitivity (B. A. J. Sarver and J. M. Good, unpublished data). Custom individually barcoded Illumina libraries (Meyer and Kircher 2010) were enriched and sequenced [100 bp, paired end (PE)] at the University of Utah Microarray and Genomic Analysis Core (HiSequation 2000), the University of Oregon Genomics and Cell Characterization Core Facility (HiSequation 2500), and the USC Epigenome Center (HiSequation 2000 and NextSequation 500). We mapped quality-filtered reads to the mouse reference genome (GRCm38) using Burrows–Wheeler Aligner v0.7.12 (Li and Durbin 2009), called variants using HaplotypeCaller in the Genome Analysis Toolkit v3.3.0 (McKenna *et al.* 2010), filtered variants on a minimum quality score of 30 and depth of 10 reads, and combined variants using VCFtools v0.1.12b (Danecek *et al.* 2011). The combined set of SNPs was filtered to include sites called across all samples. We then used a concatenated alignment of all variant genotypes to estimate a maximum likelihood phylogeny using RAxML v8.2.3 (Stamatakis 2014).

Animal use was approved by USC or UM Institutional Animal Care and Use Committees. Experimental males were weaned at ~21 days after birth and individually caged for at least 15 days to mitigate potential reproductive influences associated with dominance interactions (Snyder 1967). All experimental males were killed between 60 and 90 days using CO_2 followed by cervical dislocation (UM protocol 002-13) or only cervical dislocation (USC protocol 11394).

Transcriptome and methylome sample preparation and sequencing

We used FACS to enrich individual cell populations from across the developmental timeline of spermatogenesis following Getun *et al.* (2011). Testes were dissected following euthanasia, decapsulated, and seminiferous tubules were digested. Cells were washed repeatedly, stained with Hoechst 33343 (Invitrogen) and propidium iodide, filtered twice through a 40-μm cell strainer, and kept on ice prior to sorting. Cell sorting was performed on a FACSAria IIu cell sorter (BD Biosciences) at the UM Center for Environmental Health Sciences Fluorescence Cytometry Core. Cell populations were sorted based on size, granularity, and fluorescence and collected in 15 μl β-mercaptoethanol (Sigma, St. Louis, MO) per milliliter of RLT lysis buffer (Qiagen, Valencia, CA). RNA was extracted from each cell population using the Qiagen RNeasy kit and quantified using a Bioanalyzer 2000 (Agilent, Santa Clara, CA). Samples with RNA integrity (RIN) ≥8 were prepared for RNA-seq using the Illumina Truseq Sample Prep Kit v2 in a design that avoided batch effects between cell populations and genotypes. Libraries were sequenced [100 bp PE and 100 bp, single end (SE)] on Illumina machines at the QB3 Vincent J. Coates Genomics Sequencing Laboratory at University of California, Berkley (HiSequation 2000), the University of Utah Microarray and Genomic Analysis Core (HiSequation 2000), the University of Oregon Genomics and Cell Characterization Core Facility (HiSequation 2500), and the USC Epigenome Center (HiSequation 2000 and NextSequation 500).

For BS-seq, sperm were isolated from caudal epididymes by incubating diced tissue in 50 μl of equilibrated M199 for 40 min at 5% CO_2 at 37°. We removed tissue debris and allowed sperm to settle for 20 min. We then collected 100 μl of the top suspension and incubated the sample in 100 μl of extraction buffer (20 mM Tris Cl pH 8.0, 20 mM EDTA, 200 mM NaCl, 80 mM DTT, 4% SDS, 250 μg/ml Proteinase K) at 55°, with occasional mixing, until the sample was completely dissolved. We extracted DNA with the QIAamp DNA Mini Kit or the QIAamp DNA Blood Mini Kit (Qiagen) with a final elution in 50 μl of distilled H_2O. Bisulfite treatment, which converts unmethylated cytosines to thymine, and 100 bp PE Illumina sequencing was performed at Beijing Genomics Institute.

Illumina sequence read processing and mapping

For RNA-seq data, we removed adaptors and low-quality bases using Trimmomatic v0.32 (Bolger *et al.* 2014). Trimmed reads were mapped using Tophat v2.0.10 (default parameters) (Kim *et al.* 2013) to strain-specific (PWK/PhJ and WSB/EiJ) published pseudoreferences that incorporate all known SNPs, indels, and structural variants relative to the mouse reference genome (GRCm38) based on the classic laboratory strain,

C57BL/6J (Huang *et al.* 2014). This approach leverages the extensive annotation developed for the mouse genome while minimizing mapping bias that favors reads matching the C57BL/6J reference, which is predominantly derived from *M. m. domesticus* (Yang *et al.* 2011). We translated reads back into the GRCm38 coordinates using Lapels v1.0.5 (Holt *et al.* 2013; Huang *et al.* 2013) and counted the number of fragments uniquely mapping to protein-coding genes (GRCm38, Ensembl release 78) using featureCounts v1.4.4 (Q 20, C, primary). In addition, we counted multiple-mapped fragments within 203 multicopy/ampliconic X-linked genes (Mueller *et al.* 2013) and 156 Y-linked genes.

For methylome sequence data, we trimmed adaptors and mapped PE reads using rmapbs-pe in the RMAP package (Smith *et al.* 2008, 2009). We mapped *M. m. musculus* to GRCm38 and *M. spretus* to a custom pseudoreference generated with GATK v1.6 that combined the coordinates of GRCm38 with the sequence variation information (Sanger release version 1303) of *M. spretus* strain SPRET/EiJ (Keane *et al.* 2011).

Gene expression across spermatogenesis

All gene expression analyses were conducted using R v3.1.1(R Development Core Team 2014) and the Bioconductor v3.0 R package edgeR v3.12 (Robinson *et al.* 2010) with *P*-values adjusted to 5% false discovery rate (FDR) (Benjamini and Hochberg 1995). We restricted our analyses to protein-coding genes with greater than one fragment per kilobase of exon per million mapped reads (FPKM) in at least 4 of our 36 samples, and we also tested a range of expression thresholds (see *Results*). We evaluated library normalization using the weighted trimmed mean of *M*-values (Robinson and Oshlack 2010) or the scaling factor method (R package DESeq v1.22, Anders and Huber 2010). For brevity, we only present results using scaling factor normalization. To visualize expression data, we normalized FPKM values so that the sum of squares equals one (R package vegan v2.3-1) (Oksanen *et al.* 2015) or used variance-stabilizing transformation (Anders and Huber 2010). We plotted normalized FPKM values using the R packages beanplot v1.2 (Kampstra 2008) and gplots v2.17.0 (Warnes *et al.* 2015).

We defined a gene as "expressed" in a particular cell type (*e.g.*, spermatogonia, round spermatids) if it had an FPKM >1 in a minimum of four individuals for a given cell type. We defined a gene as "induced" in a particular cell type if the median expression in the focal cell was higher ($>2\times$) than the median expression of the other cell types combined. Similarly, we defined genes as induced at a particular stage of spermatogenesis (*e.g.*, early, late) when expression was higher ($>4\times$) than the maximum expression of all other stages (*e.g.*, Kousathanas *et al.* 2014). We used Affymetrix microarray data across 96 tissues (Mouse Genome 430 2.0 Array) from the Mouse MOE430 Gene Atlas (Su *et al.* 2002; Lattin *et al.* 2008) to identify testis-biased genes (testis expression $>2\times$ median tissue expression) and to estimate tissue specificity (τ) following the recommendations of Liao and Zhang (2006). The τ-value ranges from 0 to 1 with higher values indicative of expression restricted to one or a few tissues (Yanai *et al.* 2005; Liao and Zhang 2006; Liao *et al.* 2006).

Evolutionary analyses of protein-coding and expression divergence

We used codeml in PAML v4.7 (Yang 2007) to estimate the rate of nonsynonymous substitutions (d_N), synonymous substitutions (d_S), and the d_N/d_S ratio (ω). Annotated protein-coding sequences were extracted from published whole-genome sequences of *M. m. musculus* (PWK/PhJ), *M. m. domesticus* (WSB/EiJ), and *M. spretus* (SPRET/EiJ) (Keane *et al.* 2011). We used Biostrings v2.32.1 (Pages *et al.* 2008) to retrieve sequences from the longest transcript for each gene, excluding transcripts with internal stop codons. For genes that are induced early and late in spermatogenesis, we estimated pairwise and global (*i.e.*, one rate) ω from unrooted three-taxon alignments of (1) individual transcripts and (2) a concatenated set of transcripts for each chromosome. Estimates of d_N and d_S from one-to-one orthologs between *M. m. domesticus* (C57BL/6J) and *Rattus norvegicus* were retrieved from Ensembl Biomart release 83 (Smedley *et al.* 2015). For analyses of individual genes, we discarded transcripts with d_S values above the 95% quantile as a filter for poor alignments and transcripts with d_S estimates near zero, which are uninformative and can artificially inflate ω.

To identify differentially expressed (DE) genes between *M. m. musculus* and *M. m. domesticus*, we fit our data with negative binomial generalized linear models with Cox–Reid tagwise dispersion estimates (McCarthy *et al.* 2012). Our model included species and cell type as a single factor and we constructed a design matrix that contrasted each unique combination (*e.g.*, *M. m. musculus* spermatogonia *vs. M. m. domesticus* spermatogonia). We then tested for DE using likelihood ratio tests, dropping one coefficient from the design matrix (*i.e.*, the "null" model) and comparing that to the full model. We also calculated the correlation ($1 -$ Spearman's ρ) in chromosome-wide expression divergence between subspecies using pairwise median FPKM values with C.I.'s generated by bootstrapping the data 1000 times.

Sperm methylation divergence

We quantified sperm methylome divergence between *M. m. musculus* and *M. spretus* using BS-seq (Frommer *et al.* 1992) on eight mice (four per species). Methylation of the cytosine in cytosine–phosphate–guanine dinucleotides (CpG sites) plays a central role in the epigenetic regulation of gene expression in mammals (Reik 2007). Mammalian genomes generally show high levels of CpG methylation, punctuated by small hypomethylated regions (HMRs) associated with promoters and enhancers (Molaro *et al.* 2011). Our primary goal was to study methylation divergence at orthologous CpG sites. Therefore, we excluded sites if over half of the mapped reads for a given individual suggested a mutation resulting in the loss of CpG status (neither thymine-phosphate-guanine nor CpG). To control for differences in sequencing coverage,

we randomly downsampled uniquely mapped autosomal reads that contained at least one CpG so that individual autosomes had average CpG coverage similar to the X-linked CpGs. HMRs and other basic statistics were called using the HMR program in MethPipe (Song *et al.* 2013). Genomic windows that were called HMR in one species but not the other were flagged as potential differentially methylated regions (DMRs). We then called DMRs using the DMR program in MethPipe, requiring each DMR to contain at least five orthologous CpGs that were differentially methylated between the species based on an hypergeometric test of the four possible states (methylated *vs.* not methylated × *M. spretus vs. M. m. musculus*).

We used three different null hypotheses to test whether the proportion of X-linked DMRs differed from expectations. First, the number of X-linked base pairs divided by the total number of base pairs [minus mitochondrial DNA (mtDNA) and chromosome Y (chrY); 171,032,299/2,633,777,672 = 0.065] in the sequenced mouse genome (GRCm38) provided a crude expectation of the proportion of X-linked DMRs. Second, because hypomethylation tends to cluster near protein-coding genes, we calculated the null expectation based on the proportion of protein-coding genes that are X linked (869/19,720 = 0.044). Third, to further account for potential differences in CpG sequencing coverage between the X chromosome and the autosomes, we calculated the X-to-autosome ratio of CpGs that were covered at least 3× in one species and at least 4× in the other (the minimum number of reads necessary to detect a significantly differentially methylated CpG) among the downsampled reads (348,647/9,968,595 = 0.035).

Data availability

The data reported in this paper are available through the National Center for Biotechnology Information under accession nos. SRP065082, SRP065034, SRP075865 and SRP077631.

Results

Phylogenetic relationship of the mice used in this study

We estimated a maximum likelihood phylogeny using whole genome and targeted exome resequencing data from the mouse strains used in this study (Figure 1). The resulting tree conformed to the expected evolutionary relationships among strains of *M. m. musculus*, *M. m. domesticus*, and *M. spretus*. Strains within a given taxon are closely related and approximate levels of individual variation follow general expectations for these species and subspecies. Likewise, *M. musculus* and *M. spretus* were separated by about twice as much genetic divergence as *M. m. musculus* and *M. m. domesticus*. Thus, the different strains of mice used within our studies of expression, DNA methylation, and protein-coding divergence represent closely related samples from these three lineages.

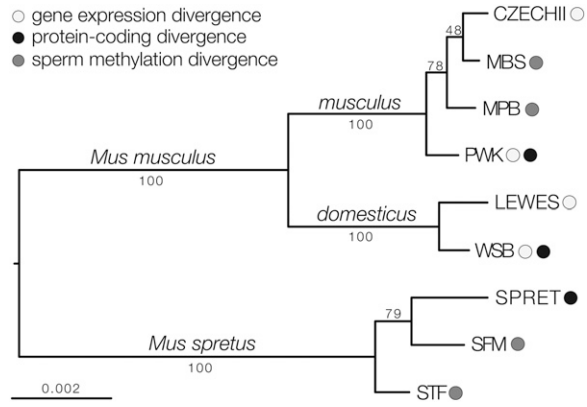

Figure 1 Evolutionary relationships among mouse strains and species. The phylogeny was estimated using maximum likelihood, based on genome-wide data. Bootstrap proportions are indicated for each internal branch. Shaded circles indicate which strains were used for estimates of gene expression, protein-coding, and sperm DNA methylation divergence.

Stage-specific dissection of gene expression across mouse spermatogenesis

We used FACS to generate highly enriched populations of four cell types spanning three phases of spermatogenesis (Supplemental Material, Figure S1, Figure 2A): (1) spermatogonia (mitosis), (2) leptotene/zygotene spermatocytes (meiosis, prior to MSCI), (3) diplotene spermatocytes (meiosis, after MSCI), and (4) round spermatids (postmeiosis). For each subspecies, *M. m. musculus* and *M. m. domesticus*, we mapped between 53 and 74 million unique sequencing fragments from each cell type to their respective genomes (Table S1). Each cell population had a distinct expression profile, there was strong clustering of transcription levels by cell type, and expression patterns of established cell- or stage-specific genes were specific to their cell type (Figure S2). Overall, these results indicate that our FACS experiments yielded highly enriched cell populations with low variance among individual samples.

We detected expression of 14,223 protein-coding genes across spermatogenesis. Most genes were expressed in multiple cell types (Table 1), but often with large between-cell differences in expression levels. Our developmental timeline brackets the onset of MSCI (at midpachytene), and as expected, we observed chromosome-wide repression of X-linked genes in diplotene spermatocytes and partial reactivation of the X chromosome in postmeiotic round spermatids (Figure 2). Each cell population produced distinct expression profiles (Figure S2), but early cell types (spermatogonia and leptotene/zygotene spermatocytes) showed very similar patterns of expression. Therefore, we grouped results into three expression stages relative to MSCI: (1) expressed early in spermatogonia and/or leptotene/zygotene spermatocytes and silenced at MSCI; (2) expressed early, silenced at MSCI, and reactivated late; and (3) expressed only late (Figure 3). Genes induced at each of these stages showed

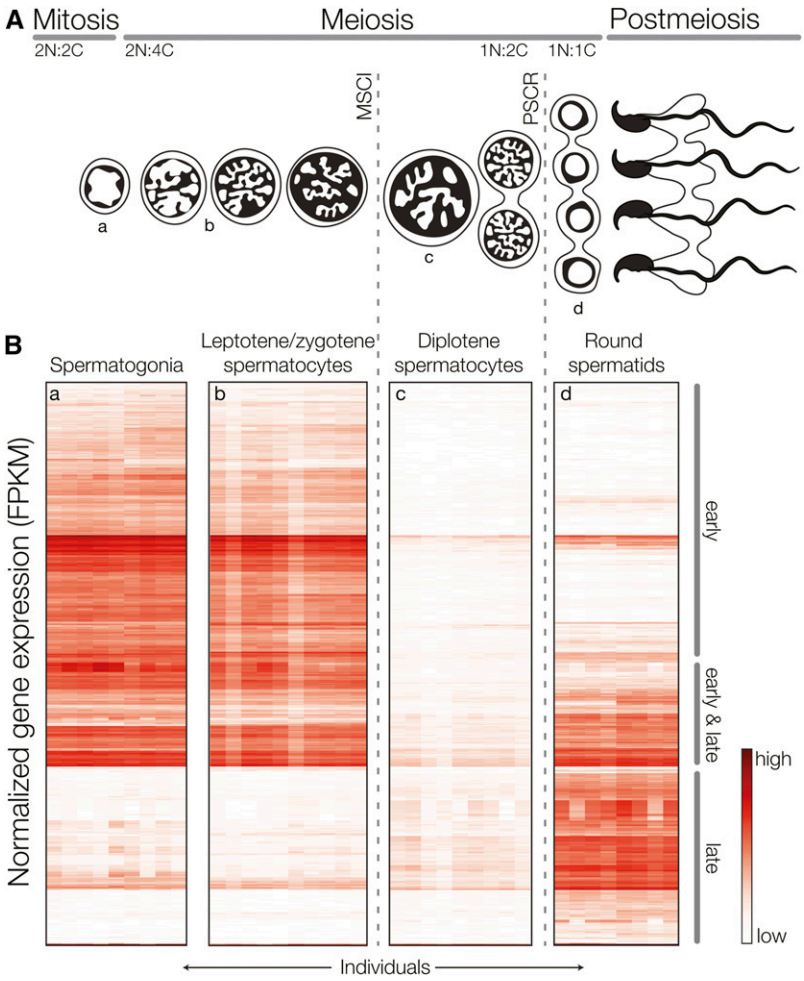

Figure 2 X-linked expression across spermatogenesis in *M. m. musculus* and *M. m. domesticus*. (A) Progression of dividing germ cells during spermatogenesis. In early prophase I the X chromosome is transcriptionally silenced (MSCI) for the remainder of meiosis and remains partially inactivated (PSCR) during postmeiotic development of spermatids. We used FACS to isolate cell populations spanning these three phases of spermatogenesis (a–d). (B) Patterns of X-linked gene expression in FACS isolated cell populations. Genes (rows) are grouped by the timing of induction: early (expressed prior to MSCI), early and late (inactivated at MSCI and reactivated late), and late (expressed only in postmeiotic cells).

good overall agreement between functional annotations and developmental processes indicative of that stage of spermatogenesis (Table 1). We also observed very high gene-by-gene correspondence between our general groupings and previously described patterns of X-linked expression during spermatogenesis (Figure S3), which used different methods of cell enrichment and expression profiling (Namekawa *et al.* 2006). These results indicate that our FACS-based enrichment captures the dynamic changes in transcription across spermatogenesis.

Next, we combined our data with published multitissue expression data and found that testis-biased genes made up a larger proportion of the genes induced late in spermatogenesis (early 4.0%, late 35.4%), consistent with increasing gene specificity during postmeiotic development (Schultz *et al.* 2003). The tissue specificity of gene expression (τ) also increased late (median $\pm$ SE τ early, 0.831 $\pm$ 0.005; late, 0.903 $\pm$ 0.009, Wilcoxon test $P \leq 0.001$). This pattern was particularly striking on the X chromosome where nearly half of late-induced genes were also testis-biased (Table 1). In addition, the X chromosome was enriched for genes induced early. These results are in agreement with previous studies indicating that X-linked gene content has been shaped by natural selection for spermatogenic genes expressed before or after MSCI (Khil *et al.* 2004; Mueller *et al.* 2008; Sin *et al.* 2012).

Faster-late and faster-X protein evolution

We calculated rates of protein-coding evolution (ω) between *M. m. musculus*, *M. m. domesticus*, and *M. spretus* for genes induced at different stages of spermatogenesis. These contrasts revealed two striking patterns. First, late-induced autosomal and X-linked genes evolved more rapidly than early-induced genes (*i.e.*, faster-late, Figure 4A, Table 2), confirming a previous finding of a positive correlation between rates of protein evolution and timing of expression during spermatogenesis (Good and Nachman 2005). Second, X-linked genes showed significantly higher ω when compared to autosomal genes (*i.e.*, faster-X, Figure 4A). These patterns of faster-late and faster-X protein evolution held when considering only pairwise differences within *M. musculus* (*M. m. musculus vs. M. m. domesticus*) (Table S2) or when considering much more divergent contrasts between the house mouse and the Norwegian rat (Table 2). They were also robust to different expression level thresholds (Table S3).

Interpreting patterns of ω requires consideration of the synonymous (d_S) and nonsynonymous (d_N) per site substitution rates in isolation. The mammalian X chromosome has

Table 1 The X chromosome is enriched for genes induced before and after MSCI and for testis-biased genes

	% Expressed[a]		% Induced[b]		% Testis-biased[c]		Functional annotation
	Auto	X	Auto	X	Auto	X	Auto and X
By cell							
Spermatogonia	54.3	50.5	19.1	40.3***	5.6	11.3***	Cell, intracellular, anatomical structure development, biosynthetic process, nucleic acid binding transcription factor activity[d]
Leptotene/zygotene spermatocytes	52.7	45.6	15.3	34.0***	5.2	7.5	Organelle, intracellular, cell, cellular nitrogen metabolic process, nucleus[d]
Diplotene spermatocytes[e]	48.0	13.2	16.2	—	48.4	—	Cilium, reproduction, microtubule organizing center
Round spermatids	50.3	35.6	22.8	23.0	42.5	44.9	Cilium, reproduction
By stage							
Early	NA	NA	10.6	33.9***	3.1	7.5***	Anatomical structure development, immune system process, plasma membrane, signal transduction, cell differentiation[d]
Early and late	NA	NA	2.3	9.3	14.3	19.5	Anatomical structure development, cytoskeletal organization, cytoskeletal protein binding, cell differentiation, cytoskeleton[d]
Late	NA	NA	7.9	19.1***	35.6	49.4***	Reproduction, signal transducer activity, extracellular region, cell wall organization or biogenesis, neurological system process

Values represent the percentage of genes that meet a given expression threshold in each cell type and stage of spermatogenesis. Enrichment of X-linked genes are based on chromosome-wise hypergeometric tests, FDR-corrected *P*-values: *** $P \leq 0.001$.

[a] Expressed, genes with FPKM > 1 in a minimum of four individuals for a given cell type out of the total genes detected (14,223 genes).

[b] Induced, by cell: genes with a median FPKM $> 2\times$ the median FPKM of all other cell types combined out of the total genes expressed. By stage: genes with a maximum FPKM $> 4\times$ the maximum FPKM of all other stages combined of the total genes expressed. (Note: a gene can be induced in more than one cell type, but can only be induced at a single stage).

[c] Testis-biased, genes with higher expression in the testes compared 96 other tissues from the Mouse MOE430 Gene Atlas out of the total genes induced.

[d] Only the top five gene enrichment categories are listed.

[e] Due to MSCI there are too few genes expressed in diplotene spermatocytes to report X-linked induced genes.

a lower per-nucleotide mutation rate than the autosomes as a consequence of male-driven molecular evolution (Ellegren and Parsch 2007). Consistent with this, we observed lower d_S for X-linked genes across all evolutionary contrasts (Table 2, Table S2) and for X-linked genes expressed early or late in spermatogenesis (Table S2). The X chromosome is also predicted to have a lower N_e relative to the autosomes and thus shallower coalescent depths on average, which could have a particularly strong impact on the comparison of X *vs.* autosomal divergence between closely related lineages. Consequently, we observed the greatest difference in X-linked *vs.* autosomal estimates of d_S between *M. m. musculus* and *M. m. domesticus* ($d_S^X/d_S^{auto} = 0.572$ *vs.* $d_S^X/d_S^{auto} \sim 0.8$ for contrasts involving *M. spretus* or rat). Finally, we found that the X chromosome shows higher d_N compared to the autosomes (Table 2), with the greatest difference among genes induced late in spermatogenesis (Table S2). Thus, we found consistently faster-late and faster-X protein-coding evolution for mouse spermatogenic genes across different levels of evolutionary divergence and when considering both relative and absolute rates of nonsynonymous divergence.

Slower-late and slower-X expression evolution

We observed strikingly different patterns of expression divergence relative to protein evolution. Although there was a general trend toward more DE genes induced late in spermatogenesis (24% of spermatogonia genes *vs.* 37% of round spermatids genes were DE) this trend was restricted to autosomal genes and there were actually fewer X-linked DE genes induced late (*i.e.*, slower-X, Figure 4, B and C). The slower-X pattern late in spermatogenesis was robust to different temporal classifications (Table S4), different expression thresholds (Table S5), different methods of accounting for X-linked ampliconic/multicopy genes (Figure S4), and was also apparent in per-chromosome comparisons (Figure 5). As discussed above, testis-biased genes tended to be expressed late in spermatogenesis (Table 1). When we restricted our analysis to testis-biased genes, we found that expression divergence was dramatically reduced late and was similarly constrained between the X chromosome and the autosomes (*i.e.*, slower-late, Figure 4B). If we compare expression divergence on the autosomes and the X chromosome while excluding testis-biased genes, the pattern of slower-X late is even more

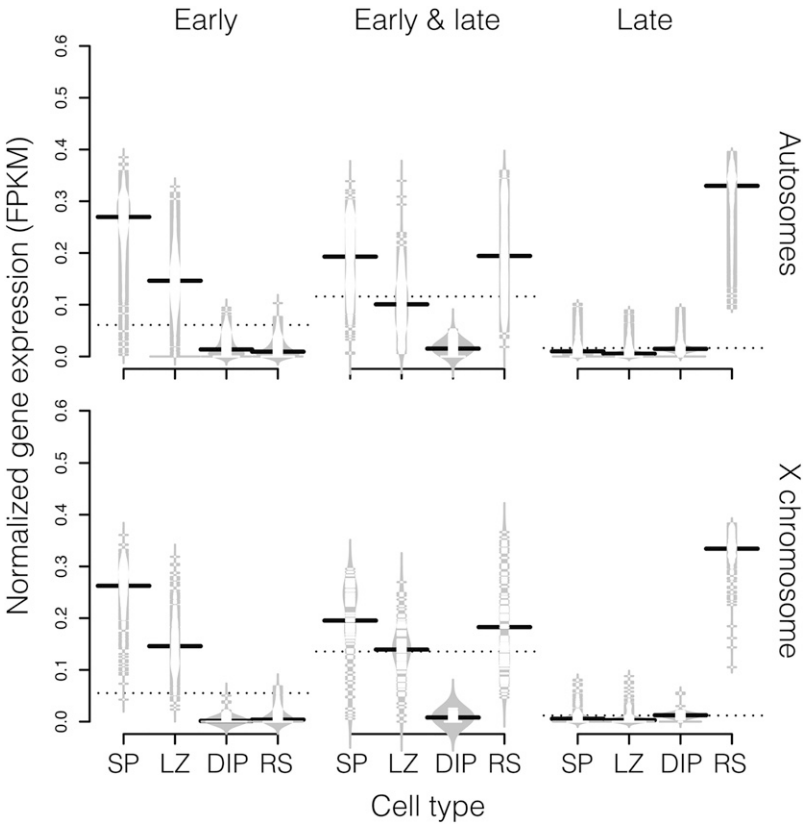

Figure 3 Expression patterns for genes induced at different stages of spermatogenesis in *M. musculus*. The normalized FPKM values for each gene is plotted as a horizontal tick mark and the distribution density for each cell type is plotted as a gray outline. Lines represent the median FPKM for each cell type (solid) and stage of spermatogenesis (dashed). Genes induced early have higher expression before the onset of MSCI (LZ, leptotene/zygotene spermatocytes and SP, spermatogonia). Genes induced both early and late are silenced at MSCI (DIP, diplotene spermatocytes) and are reactivated in postmeiotic cells (RS, round spermatids). Genes induced late are only highly expressed in postmeiotic cells.

apparent (Figure S5). Thus, slower-late expression evolution appears to be a general feature of X-linked spermatogenic genes, but was restricted to testis-biased genes on the autosomes.

These estimates of differential expression reflect divergence of a biochemical phenotype that do not account for the potential impacts of lower mutation rates and/or shallower coalescent times on the X chromosome. If we conservatively scale our expectation for X-linked differential expression by the X-to-autosome ratio of synonymous divergence ($d_S^X/d_S^{auto} = 0.572$ for the contrast between *M. m. musculus* and *M. m. domesticus*) then we find that the X chromosome becomes significantly enriched for DE genes induced early ($P < 0.001$) and the slower-X pattern becomes nonsignificant late ($P = 0.38$). Likewise, for testis-biased genes, the X chromosome is significantly enriched for DE genes early ($P < 0.001$) but not late ($P = 0.924$). Thus, the strongest pattern in our data is that expression divergence changes considerably across spermatogenesis both on and off the X chromosome, but at each stage the rate of evolution of the X chromosome relative to the autosomes depends on the extent to which mutation and effective population size influence evolution of this phenotype.

Overall patterns of protein divergence and expression divergence were qualitatively different across this timeline. Protein divergence increased late in spermatogenesis and was elevated on the X chromosome, while the opposite was true for expression divergence. Interpretation of X *vs.* autosomal expression divergence is clearly dependent on the assumptions one makes with respect to null expectations. Given this, it is informative to focus on the relationships between gene expression and protein evolution across spermatogenesis. We calculated correlations and partial correlations between protein evolution (ω), expression level (normalized FPKM), log2 fold change between subspecies (logFC), and tissue specificity (τ) (Figure S6). There was a strong positive relationship between expression level and logFC on and off the X chromosome for genes induced early and late in spermatogenesis. LogFC and τ were positively correlated on the autosomes early, indicating that tissue-specific genes tended to also show larger changes in expression levels between *M. m. musculus* and *M. m. domesticus*. In contrast, logFC was negatively correlated with both τ and ω on the autosomes late in spermatogenesis, but only when testis-biased genes were included (Figure S6). These results support our general finding of elevated protein-coding divergence coupled with more constrained gene expression for testis-biased genes late in spermatogenesis.

Slower-X sperm methylome evolution

For BS-seq, we obtained an average genomic coverage of 12.7× in *M. m. musculus* and 12.3× in *M. spretus* (Table S6, Table S7). Methylation levels across individual CpG sites were most strongly correlated among individuals within strains, followed by strains within species, followed by between-species comparisons (Table S8), as expected based on patterns of DNA sequence divergence (Figure 1). Approximately 6.0% of the genome lies underneath X-linked HMRs, which is reasonably

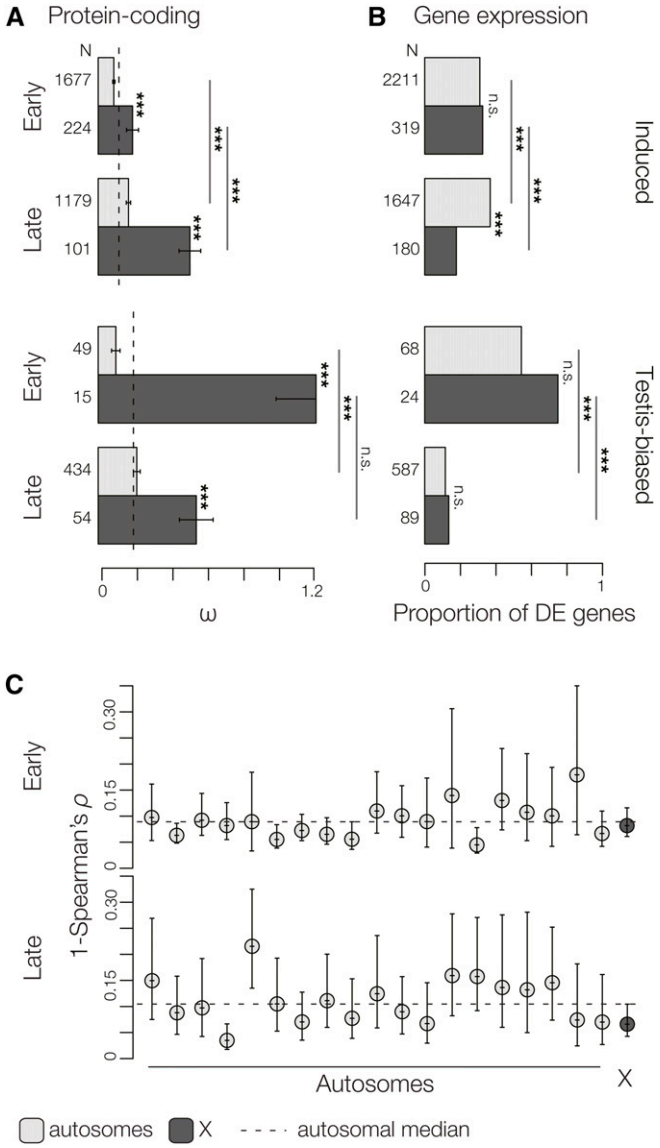

Figure 4 Evolutionary divergence in protein-coding sequence and expression level. (A) Median (±SE) estimates of protein-coding divergence (ω) among subspecies of *M. musculus* and *M. spretus* is higher for genes induced late and for X-linked genes. Gene expression divergence between subspecies of *M. musculus* estimated as (B) the proportion of induced genes that are DE and (C) the pairwise correlations of gene expression per chromosome ($1 - \rho$, ± 95% C.I.). The evolution of X-linked genes is either equivalent or slower than autosomal genes and there is a marked drop in the proportion of testis-biased genes induced late in spermatogenesis that are DE. *N* = total number of genes. Significant differences in ω (Wilcoxon test) and proportion of DE genes (χ^2) are indicated for each contrast. FDR-corrected *P*-values: *** $P \leq 0.001$.

close to expectations based on the relative length of the X chromosome (6.4%). We defined methylome divergence by identifying DMRs as genomic regions with adequate coverage in both species but where an HMR was called in only one of the species. Only 2.3% of the 9580 DMRs between *M. m. musculus* and *M. spretus* were X linked, a strongly significant reduction given the proportion of X-linked CpGs ($\chi^2 = 23.2$, $P < 10^{-5}$; Figure 6, Table S9). We observed considerable variation in DMR enrichment among chromosomes (Figure 6), likely because of the sensitivity of enrichment tests when sample sizes are large. Nine of 20 linkage groups showed significant skews in observed *vs.* expected DMRs but the X chromosome always showed the strongest de-enrichment of DMRs across a range of test configurations. We emphasize here that we downsampled autosomal reads to match X-linked coverage; therefore, our results cannot be explained by differential coverage. Our results remained qualitatively identical across five different downsampling schemes. Thus, in mouse sperm, the X chromosome shows less absolute divergence in sperm DNA methylation status relative to the autosomes.

Finally, we evaluated the potential influence of lower X chromosome substitution rates on sperm methylome evolution. Similar to our expression analyses above, we corrected our expectation for the number of X-linked DMRs by the X-to-autosome ratio of synonymous substitutions ($d_S^X/d_S^{auto} = 0.77$ for the contrast between *M. m. musculus* and *M. m. spretus*). Using this correction, the reduction in the frequency of DMRs on the X chromosome becomes nonsignificant (χ^2, $P = 0.088$).

Discussion

Forty years ago, King and Wilson argued that protein sequence and gene expression represent distinct levels of evolution (King and Wilson 1975). This influential paper popularized the ideas that evolution proceeds through different molecular mechanisms along the transition from genotype to phenotype and that gene expression may play a predominant role in organismal evolution. In our study we found striking contrasts in patterns of divergence between different forms of molecular evolution dependent on chromosome origin and developmental stage of spermatogenesis. Our cell-specific data yield new insights into the evolution of spermatogenesis and the critical role that developmental context plays in molecular evolution on and off the sex chromosomes. Below we discuss the implications of our results for the evolution of spermatogenesis, the X chromosome, and speciation.

Protein evolution and spermatogenesis

Faster-X protein evolution has now been found across a broad range of taxa, including mammals (Hvilsom *et al.* 2012; Veeramah *et al.* 2014), birds (Mank *et al.* 2007), flies (Begun *et al.* 2007; Langley *et al.* 2012; Garrigan *et al.* 2014), and other insects (Jaquiery *et al.* 2012; Sackton *et al.* 2014). Both higher rates of adaptive substitutions (Kousathanas *et al.* 2014) and relaxed constraint (Wright *et al.* 2015) likely contribute to these patterns. X-linked sequence evolution is not always unusual (reviewed in Vicoso and Charlesworth 2006; Ellegren and Parsch 2007; Meisel and Connallon 2013), but there is strong support for faster-X protein evolution for genes expressed in male reproductive tissues (Torgerson and Singh 2003, 2006; Baines *et al.* 2008; Grath and Parsch 2012; Sin *et al.* 2012; Kousathanas *et al.* 2014). From these data, gene expression has emerged as a

Table 2 Protein-coding divergence on the X chromosome and the autosomes

	Global estimates among *Mus* species	*M. m. domesticus vs. R. norvegicus*
N		
Auto	9898	10,565
X	416	311
ω		
Auto	$0.114 \pm 3.00 \times 10^{-3}$	$0.119 \pm 1.61 \times 10^{-3}$
X	$0.235^{***} \pm 2.82 \times 10^{-2}$	$0.192^{***} \pm 1.33 \times 10^{-2}$
d_N		
Auto	$0.003 \pm 5.48 \times 10^{-5}$	$0.023 \pm 3.38 \times 10^{-4}$
X	$0.004^{***} \pm 4.99 \times 10^{-4}$	$0.029^{***} \pm 2.82 \times 10^{-3}$
d_S		
Auto	$0.024 \pm 1.10 \times 10^{-4}$	$0.196 \pm 5.73 \times 10^{-4}$
X	$0.018^{***} \pm 4.90 \times 10^{-4}$	$0.156^{***} \pm 3.52 \times 10^{-3}$
d_S^X/d_S^{auto}	0.750	0.796

Estimates of median (±SE) omega (ω), nonsynonymous substitution rate (d_N), and synonymous substitution rate (d_S) among *M. m. musculus*, *M. m. domesticus*, *M. spretus*, and *R. norvegicus*. *N* = the number of genes in each comparison. Significant differences (Wilcoxon test) between the autosomes and X chromosome are indicated by FDR-corrected (Benjamini and Hochberg 1995) *P*-values: *** $P < 0.001$.

defining factor in faster-X protein evolution, with breadth of expression, tissue specificity, and degree of sex bias all strongly influencing evolutionary rates (Meisel 2011; Meisel *et al.* 2012b).

Given these general findings, the details of spermatogenesis should strongly dictate patterns of molecular evolution on and off the sex chromosomes, yet most evolutionary studies have not utilized a strong developmental framework (but see Kousathanas *et al.* 2014). Our FACS data allowed us to partition genes across spermatogenesis, yielding strong support for faster-X protein evolution (Figure 4A) based on relative (ω) and absolute (d_N) estimates of amino acid divergence. Faster-X protein evolution was most striking when considering ω estimates that used d_S to approximate neutral divergence. This assumption is violated in many species due to selection for biased codon usage. For example, the X chromosome shows stronger codon usage bias in *Drosophila* (Singh *et al.* 2005), which in turn may inflate X-linked estimates of ω (Campos *et al.* 2013). There is also weak codon usage bias in mice, but unlike *Drosophila*, it is significantly weaker on the X chromosome (Kessler and Dean 2014) and therefore conservative with respect to the observation of faster-X protein evolution. Further, both lower mutation rates and shallower coalescent times likely contribute to less nucleotide divergence on the mouse X chromosome (Table S2), making the observation of higher X-linked d_N conservative.

Some aspects of our faster-X protein-coding results are seemingly contrary to the basic dominance predictions of faster-X theory. Postmeiotic cells are haploid, leading to the prediction that faster-X evolution in the germ line should be restricted to genes expressed prior to meiosis (Kousathanas *et al.* 2014). However, spermatids form a multicellular syncytium connected through intercellular bridges that enable functional equivalence through cytoplasmic exchange (Braun *et al.* 1989; Caldwell and Handel 1991). Exchange of gene products between spermatids is likely a functional necessity given that many sex-linked genes are essential to the postmeiotic stages of spermatogenesis. Assuming exchange of autosomal gene products maintains functional diploidy, then our finding of faster-X protein evolution across the diploid and haploid stages of spermatogenesis is generally consistent with the dominance predictions of faster-X theory (Charlesworth *et al.* 1987; Vicoso and Charlesworth 2009).

Regulatory evolution and spermatogenesis

In contrast to protein evolution, X-linked postmeiotic genes (*i.e.*, induced late) showed less differential expression than comparable autosomal genes (Figure 4). As with expression divergence, sperm methylome evolution also appeared slower on the X chromosome (Figure 5). Given the strong signature of faster-X protein evolution, why do we find evidence for equivalent or slower-X gene expression and DNA methylation evolution across the same developmental timeline? One simple explanation is that one or more of the assumptions of the faster-X model sequence evolution do not hold for these complex biochemical traits. First, for the predictions of faster-X theory to hold, these regulatory phenotypes must reflect linked-sequence evolution. For faster-X expression divergence, this would require that differences in transcript abundances are due to divergence in *cis*-regulatory elements and/or X-linked *trans*-regulatory elements (Kayserili *et al.* 2012; Meisel *et al.* 2012a; Meisel and Connallon 2013). Several studies suggest that divergence in transcript abundances is largely determined by evolution in *cis* (Wittkopp *et al.* 2004; Landry *et al.* 2005; Wittkopp *et al.* 2008; Graze *et al.* 2009; Goncalves *et al.* 2012; Shi *et al.* 2012; Shen *et al.* 2014; Mack *et al.* 2016), while other research indicates that *trans*-regulatory divergence is more common (Emerson *et al.* 2010; McManus *et al.* 2010; Schaefke *et al.* 2013; Coolon *et al.* 2014; Meiklejohn *et al.* 2014; Combes *et al.* 2015) or that the inferred mode of regulatory divergence is dependent on taxon and experimental design (Coolon and Wittkopp 2013; Guerrero *et al.* 2016). The mechanisms underlying the evolution of DNA methylation are even more poorly understood, but levels of DNA methylation within a given genomic region appear strongly

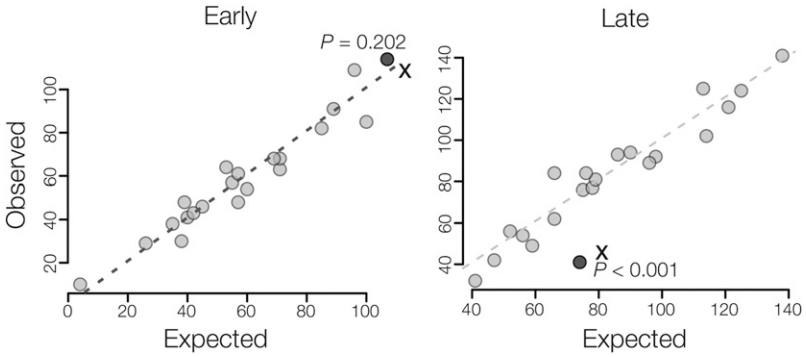

Figure 5 Contrasting patterns of gene expression divergence on the X chromosome. Early in spermatogenesis the X chromosome has a similar proportion of DE genes compared to the autosomes, while there are fewer X-linked DE genes late in spermatogenesis. The shift in the number of observed/expected X-linked genes between early and late reflects the enrichment of X-linked genes induced early. Significance is based on chromosome-wise hypergeometric test for enrichment with FDR-corrected *P*-values.

dependent on underlying (*i.e.*, *cis*) genetic sequences (Hernando-Herraez *et al.* 2015).

Faster-X sequence evolution also assumes that beneficial mutations are on average at least partially recessive (Charlesworth *et al.* 1987), while theory (Gibson and Weir 2005) and several empirical studies (Lemos *et al.* 2008; McManus *et al.* 2010; Schaefke *et al.* 2013) suggest that *cis*-regulatory elements should on average act additively. Nonetheless, these studies also find a substantial proportion of *cis*-regulatory elements that act nonadditively or, in some cases, a greater overall proportion of nonadditive *cis*-regulatory elements (Coolon *et al.* 2014). Unfortunately, these issues remain largely unresolved on the X chromosome because both dominance relationships and *cis*- *vs.* *trans*-regulatory evolution are usually assessed through allele-specific expression in F_1 genotypes, which cannot be evaluated for X-linked genes during spermatogenesis.

It is also important to consider what fraction of X-linked substitutions that influence gene expression or DNA methylation reflect new mutations that have been targeted by positive directional selection. One formal possibility is that divergence of regulatory traits simply reflects neutral sequence evolution. Both patterns of slower-X gene expression and methylation divergence become nonsignificant when expectations are corrected by lower synonymous substitution rates on the X chromosome. This simple correction is likely highly conservative, but does suggest that differences in mutation rates and/or the effective population sizes may partially account for patterns of divergence on the X chromosome. We still lack a strong theoretical framework for differentiating between adaptive and neutral divergence of expression phenotypes (Khaitovich *et al.* 2005b; Meisel and Connallon 2013). Recent genomic analyses of patterns of sequence polymorphism and divergence in mice indicate widespread adaptive evolution of both coding (Halligan *et al.* 2010) and noncoding regions (Halligan *et al.* 2011, 2013). Most putatively adaptive autosomal substitutions in mouse genomes occur within candidate regulatory regions (*i.e.*, untranslated exons and conserved noncoding elements), although the individual fitness effects of amino acid substitutions appear to be much larger (Halligan *et al.* 2013). These studies did not consider X-linked patterns directly but do suggest that a substantial fraction of substitutions within regulatory regions may be targeted by positive selection. However, if selection on gene expression acts on standing genetic variation, as opposed to new mutations, then substitution rates are predicted to be lower on the X chromosome (Meisel and Connallon 2013), given lower levels of X-linked genetic diversity in mice (Geraldes *et al.* 2008). The relative contribution of new mutations *vs.* standing genetic variation to adaptive regulatory divergence has not yet been explicitly addressed (Coolon and Wittkopp 2013).

In sum, it is clear that extending the faster-X model sequence evolution to regulatory phenotypes depends on several assumptions that are both restrictive and remain largely unresolved. However, if regulatory divergence between subspecies of mice were simply a consequence of the genetic architecture of these traits, mutational processes, or the origin of adaptive variation, then we might reasonably expect patterns on and off the X chromosome to be consistent across different stages of spermatogenesis. Instead we found that X-linked expression divergence, both overall and relative to the autosomes, changed dynamically over the timeline of spermatogenesis with a strong signature of less divergence late (Figure 4B). Given this finding, we propose that slower-late regulatory evolution may be best explained by strong developmental constraints on gene expression phenotypes during the later stages of spermatogenesis that are particularly acute on the sex chromosomes.

Evolution of the mammalian X chromosome likely reflects a balance between the inherent constraints of dosage compensation (Ohno 1967; Kohn *et al.* 2004) and spermatogenesis (Schultz *et al.* 2003; Shima *et al.* 2004; Chalmel *et al.* 2007) with the conflicting forces of sexual and antagonistic selection that favor X-linked male-biased genes (Rice 1984). During spermatogenesis, the sex chromosomes are tightly regulated through the generally repressive epigenetic environments of MSCI and PSCR (Turner 2007; Hu and Namekawa 2015). For example, PSCR in mice is partially maintained by the multicopy Y-linked *Sly* gene (Cocquet *et al.* 2009, 2010). *Sly* represses postmeiotic sex chromosome expression and favors Y transmission in spermatids. The multicopy X-linked genes *Slx/Slxl1* seem to counter this by increasing sex chromosome expression and X transmission. This direct antagonism appears to have driven a copy-number arms race (Scavetta and Tautz 2010; Ellis *et al.* 2011) where each added copy leads to an incremental

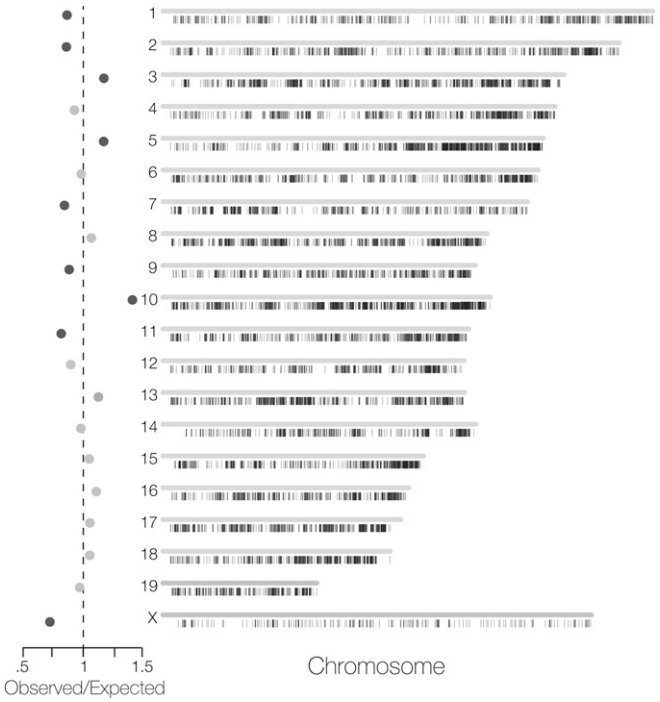

Figure 6 Evolution of the mouse sperm methylome. Chromosomal distributions of DMRs between *M. m. musculus* and *M. spretus*. The observed and expected numbers of DMRs are plotted to the left. Expectations are based on the proportion of CpG sites on each chromosome multiplied by the total number of DMRs. Darkly shaded chromosomes have significantly more or less DMRs than expected based on chromosome-wise hypergeometric tests. The X chromosome has significantly fewer DMRs compared to all of the autosomes ($P < 0.001$).

increase in relative expression and subsequent counterselection for upregulation of the other gene group (Cocquet *et al.* 2012). So while the underlying genomic architecture evolves rapidly via gene duplication (Ellis *et al.* 2011), expression level phenotypes appear to be under strong stabilizing selection for a dosage equilibrium between sex-linked postmeiotic genes that if disrupted leads to male sterility. This is evidence for strong constraint on the regulatory phenotypes of X-linked genes that overcome PSCR to be expressed during this critical period of sperm development. Our data suggest that such constraints likely extend more broadly across the X chromosome and to testis-biased autosomal genes.

We also found that patterns of DNA methylation diverged more slowly on X chromosomes compared to the autosomes (Figure 5). Dynamic methylation plays a key role in mammalian genome regulation (Li *et al.* 1992; Okano *et al.* 1999; Reik *et al.* 2001), yet very little is known about either the tempo or mechanisms of DNA methylome evolution. Sperm are the first mature cells following a major "erasure"; nearly the entire genome is demethylated in spermatogonia stem cells and then remethylated late in spermatogenesis (Reik *et al.* 2001). A study involving primates found the methylomes of mature sperm to differ from those of somatic cells in several important ways. Most notably, the HMRs are more numerous and extend for longer genomic intervals in sperm compared to somatic cells (Molaro *et al.* 2011). We propose that the observation of less X-linked sperm methylome divergence may be an extension of the same regulatory constraints that lead to slower gene expression divergence late in spermatogenesis, as well as other X-linked phenomena such as mutational environment. Comparable methylome data from other tissues and other stages in spermatogenesis will be helpful in resolving these outstanding questions.

Cis-regulatory evolution is thought to proceed with fewer pleiotropic constraints than protein-coding divergence (*e.g.*, Carroll 2008). However, our results indicate that the stages of spermatogenesis that show the fastest rates of protein evolution show less expression divergence for both X-linked and testis-biased genes. Protein evolution is strongly influenced by underlying patterns of gene expression; there are generally higher rates of protein-coding divergence for genes that have lower expression (Nguyen *et al.* 2015) and for narrowly expressed genes (Liao *et al.* 2006; Meisel 2011). Expression specificity increases late in spermatogenesis and the X chromosome is enriched for testis-biased postmeiotic genes. Therefore expression specificity may be the primary factor underlying faster-late and faster-X protein evolution. While divergence in gene expression (logFC) and tissue specificity (τ) were also positively correlated early in spermatogenesis, they were negatively correlated for autosomal testis-biased genes expressed late (Figure S6). Thus, specificity may actually constrain expression divergence late in spermatogenesis, especially for postmeiotic testis-biased genes that presumably play critical roles in sperm development and maturation. There is typically a positive association between differential expression and tissue specificity (Meisel *et al.* 2012a), suggesting that our results reflect a unique feature of sperm development rather than a general molecular evolutionary trend.

Our observation of less X-linked expression divergence late in spermatogenesis differs some from studies in mammals reporting elevated (uncorrected) X-linked expression divergence primarily in testis (Khaitovich *et al.* 2005a; Zhang *et al.* 2010; Brawand *et al.* 2011). These previous studies have focused on various whole tissue contrasts spanning different taxa and phylogenetic depths. However, Zhang *et al.* (2010) did report greater relative X-linked expression divergence in spermatids between mouse and rat, the exact cell population that we found to be the most conserved between subspecies of mice (Figure 4). While this could reflect changes in X-linked expression evolution over deeper evolutionary timescales, this previous result was based on a metaanalysis of microarray data collected independently in mouse (Chalmel *et al.* 2007) and rat (Johnston *et al.* 2008) using different cell-enrichment procedures. A full assessment of testis gene expression evolution between mouse and rat awaits the comparison of cell-specific transcriptomes that control for potential experimental artifacts.

How broadly the slower-late X and testis-biased autosomal patterns of regulatory evolution apply to other taxa remains

to be seen. Expression divergence has not been systematically evaluated in nonmammalian systems using cell- or stage-specific data, making the relative contributions of cellular composition and developmental constraint difficult to determine. This technical limitation aside, the influence of developmental timing on spermatogenic expression evolution will also be dependent on the existence or extent of MSCI/PSCR-like phenomena in other taxa. For example, faster-X expression divergence has also been reported in *Drosophila* (Kayserili *et al.* 2012; Meisel *et al.* 2012a; Coolon *et al.* 2015; Llopart 2015) where the X chromosome appears to be transcriptionally repressed during spermatogenesis (Meiklejohn *et al.* 2011). Whether this repression reflects a process akin to MSCI has been contentious, but it does suggest that regulatory constraints likely play an important role in sex chromosome evolution (Vibranovski 2014).

Implications for speciation

Faster-X theory was originally proposed in part to explain two observations that invoke a large role for sex chromosomes in speciation (Charlesworth *et al.* 1987). First, when hybrids between recently diverged lineages show sex-specific sterility or inviability, it is usually the heterogametic sex (Haldane 1922). Second, heterogametic sterility is disproportionately linked to the X or Z chromosomes, a pattern known as the large-X effect (Coyne 1992). Faster-X evolution remains one of the predominant mechanisms invoked to explain the evolution of hybrid sterility (Kousathanas *et al.* 2014), and the link between rapid evolution and speciation is intuitive. A long-standing alternative hypothesis is that spermatogenesis is an inherently sensitive process that may be easily disrupted in hybrids (Lifschytz and Lindsley 1972; Jablonka and Lamb 1991; Wu and Davis 1993). Disruptions of MSCI/PSCR are strong *a priori* candidate regulatory mechanisms for the sensitivity of spermatogenesis (Lifschytz and Lindsley 1972). Studies in mice (Good *et al.* 2010; Bhattacharyya *et al.* 2013; Campbell *et al.* 2013; Turner *et al.* 2014) and other mammals (Davis *et al.* 2015) have recently found a strong link between regulatory disruption of the X chromosome during spermatogenesis and the evolution of hybrid male sterility. Our results reveal that the same developmental stages that have disrupted gene expression in mouse hybrids (Good *et al.* 2010; Bhattacharyya *et al.* 2013; Campbell *et al.* 2013) show the strongest evolutionary constraints in gene expression levels (Figure 4). While these data do not discount an important role for faster-X protein-coding evolution in speciation, they do suggest that inherent developmental constraints on the regulation of gene expression late in spermatogenesis may play a central and underappreciated role in the evolution of hybrid male sterility.

Acknowledgments

We thank Pamela K. Shaw, Irina Getun, Bivian Torres, Colin Callahan, and Brent Young for assistance with FACS and other sample preparations; Francois Bonhomme for mice; and the staff of the University of Montana (UM) Laboratory Animal Research facility. Members of the J.M.G. and M.D.D. labs gave us helpful feedback on experimental results, and comments from Bret Payseur and multiple anonymous reviewers improved previous versions of this manuscript. We thank the UM Fluorescence Cytometry Core, supported by the National Institute of General Medical Sciences of the National Institutes of Health (NIH) (P30-GM103338) and the UM Genomics Core, supported by a grant from the M. J. Murdock Charitable Trust and the Vincent J. Coates Genomics Sequencing Laboratory at the University of California, Berkeley, supported by NIH S10 instrumentation grants S10-RR029668 and S10-RR027303. This research was supported by the Eunice Kennedy Shriver National Institute of Child Health and Human Development (R01-HD073439; to J.M.G.), the National Institute of General Medical Sciences (R01-GM098536; to M.D.D.), and the National Science Foundation (1146525; to M.D.D.).

Literature Cited

Anders, S., and W. Huber, 2010 Differential expression analysis for sequence count data. Genome Biol. 11: R106.

Bachtrog, D., M. Kirkpatrick, J. E. Mank, S. F. McDaniel, J. C. Pires *et al.*, 2011 Are all sex chromosomes created equal? Trends Genet. 27: 350–357.

Baines, J. F., and B. Harr, 2007 Reduced X-linked diversity in derived populations of house mice. Genetics 175: 1911–1921.

Baines, J. F., S. A. Sawyer, D. L. Hartl, and J. Parsch, 2008 Effects of X-linkage and sex-biased gene expression on the rate of adaptive protein evolution in *Drosophila*. Mol. Biol. Evol. 25: 1639–1650.

Begun, D. J., and P. Whitley, 2000 Reduced X-linked nucleotide polymorphism in *Drosophila simulans*. Proc. Natl. Acad. Sci. USA 97: 5960–5965.

Begun, D. J., A. K. Holloway, K. Stevens, L. W. Hillier, Y.-P. Poh *et al.*, 2007 Population genomics: whole-genome analysis of polymorphism and divergence in *Drosophila simulans*. PLoS Biol. 5: e310–e326.

Benjamini, Y., and Y. Hochberg, 1995 Controlling the false discovery rate: a practical and powerful approach to multiple testing. J.R. Stat. Soc. 57: 289–300.

Bhattacharyya, T., S. Gregorova, O. Mihola, M. Anger, J. Sebestova *et al.*, 2013 Mechanistic basis of infertility of mouse intersubspecific hybrids. Proc. Natl. Acad. Sci. USA 110: E468–E477.

Bolger, A. M., M. Lohse, and B. Usadel, 2014 Trimmomatic: a flexible trimmer for Illumina sequence data. Bioinformatics 30: 2114–2120.

Braun, R. E., R. R. Behringer, J. J. Peschon, R. L. Brinster, and R. D. Palmiter, 1989 Genetically haploid spermatids are phenotypically diploid. Nature 337: 373–376.

Brawand, D., M. Soumillon, A. Necsulea, P. Julien, G. Csárdi *et al.*, 2011 The evolution of gene expression levels in mammalian organs. Nature 478: 343–348.

Caldwell, K. A., and M. A. Handel, 1991 Protamine transcript sharing among postmeiotic spermatids. Proc. Natl. Acad. Sci. USA 88: 2407–2411.

Campbell, P., J. M. Good, and M. W. Nachman, 2013 Meiotic sex chromosome inactivation is disrupted in sterile hybrid male house mice. Genetics 193: 819–828.

Campos, J. L., K. Zeng, D. J. Parker, B. Charlesworth, and P. R. Haddrill, 2013 Codon usage bias and effective population

sizes on the X chromosome *vs.* the autosomes in *Drosophila melanogaster*. Mol. Biol. Evol. 30: 811–823.
Carroll, S. B., 2008 Evo-devo and an expanding evolutionary synthesis: a genetic theory of morphological evolution. Cell 134: 25–36.
Chalmel, F., A. D. Rolland, C. Niederhauser-Wiederkehr, S. S. W. Chung, P. Demougin *et al.*, 2007 The conserved transcriptome in human and rodent male gametogenesis. Proc. Natl. Acad. Sci. USA 104: 8346–8351.
Charlesworth, B., J. A. Coyne, and N. H. Barton, 1987 The relative rates of evolution of sex chromosomes and autosomes. Am. Nat. 130: 113–146.
Charlesworth, D., 2013 Plant sex chromosome evolution. J. Exp. Bot. 64: 405–420.
Cocquet, J., P. J. I. Ellis, Y. Yamauchi, S. K. Mahadevaiah, N. A. Affara *et al.*, 2009 The multicopy gene *Sly* represses the sex chromosomes in the male mouse germline after meiosis. PLoS Biol. 7: e1000244.
Cocquet, J., P. J. I. Ellis, Y. Yamauchi, J. M. Riel, T. P. S. Karacs *et al.*, 2010 Deficiency in the multicopy *Sycp3*-like X-linked genes *Slx* and *Slxl1* causes major defects in spermatid differentiation. Mol. Biol. Cell 21: 3497–3505.
Cocquet, J., P. J. I. Ellis, S. K. Mahadevaiah, N. A. Affara, D. Vaiman *et al.*, 2012 A genetic basis for a postmeiotic X *vs.* Y chromosome intragenomic conflict in the mouse. PLoS Genet. 8: e1002900.
Combes, M. C., Y. Hueber, A. Dereeper, S. Rialle, J. C. Herrera *et al.*, 2015 Regulatory divergence between parental alleles determines gene expression patterns in hybrids. Genome Biol. Evol. 7: 1110–1121.
Coolon, J. D., and P. J. Wittkopp, 2013 cis- and trans-regulation in Drosophila interspecific hybrids, pp. 37–57 in *Polyploid and Hybrid Genomics*, edited by Z. J. Chen, and J. A. Birchler. John Wiley & Sons, New York.
Coolon, J. D., C. J. McManus, K. R. Stevenson, B. R. Graveley, and P. J. Wittkopp, 2014 Tempo and mode of regulatory evolution in *Drosophila*. Genome Res. 24: 797–808.
Coolon, J. D., K. R. Stevenson, C. J. McManus, B. Yang, B. R. Graveley *et al.*, 2015 Molecular mechanisms and evolutionary processes contributing to accelerated divergence of gene expression on the *Drosophila* X chromosome. Mol. Biol. Evol. 32: 2605–2615.
Coyne, J. A., 1992 Genetics and speciation. Nature 355: 511–515.
Danecek, P., A Auton, G Abecasis, C. AE. Albers, and Banks *et al.*, 2011 The variant call format and VCFtools. Bioinformatics 27: 2156–2158.
Davis, B. W., C. M. Seabury, W. A. Brashear, G. Li, M. Roelke-Parker *et al.*, 2015 Mechanisms underlying mammalian hybrid sterility in two feline interspecies models. Mol. Biol. Evol. 32: 2534–2546.
Dean, R., P. W. Harrison, A. E. Wright, F. Zimmer, and J. E. Mank, 2015 Positive selection underlies faster-Z evolution of gene expression in birds. Mol. Biol. Evol. 32: 2646–2656.
Eddy, E. M., 2002 Male germ cell gene expression. Recent Prog. Horm. Res. 57: 103–128.
Ellegren, H., 2007 Characteristics, causes and evolutionary consequences of male-biased mutation. Proc. Biol. Sci. 274: 1–10.
Ellegren, H., 2011 Sex-chromosome evolution: recent progress and the influence of male and female heterogamety. Nat. Rev. Genet. 12: 157–166.
Ellegren, H., and J. Parsch, 2007 The evolution of sex-biased genes and sex-biased gene expression. Nat. Rev. Genet. 8: 689–698.
Ellis, P. J. I., J. Bacon, and N. A. Affara, 2011 Association of *Sly* with sex-linked gene amplification during mouse evolution: a side effect of genomic conflict in spermatids? Hum. Mol. Genet. 20: 3010–3021.
Emerson, J. J., H. Kaessmann, E. Betrán, and M. Long, 2004 Extensive gene traffic on the mammalian X chromosome. Science 303: 537–540.
Emerson, J. J., L.-C. Hsieh, H.-M. Sung, T.-Y. Wang, C.-J. Huang *et al.*, 2010 Natural selection on *cis* and *trans* regulation in yeasts. Genome Res. 20: 826–836.
Fairfield, H., G. J. Gilbert, M. Barter, R. R. Corrigan, M. Curtain *et al.*, 2011 Mutation discovery in mice by whole exome sequencing. Genome Biol. 12: R86.
Firman, R. C., F. Garcia-Gonzalez, E. Thyer, S. Wheeler, Z. Yamin *et al.*, 2015 Evolutionary change in testes tissue composition among experimental populations of house mice. Evolution 69: 848–855.
Frommer, M., L. E. McDonald, D. S. Millar, C. M. Collis, F. Watt *et al.*, 1992 A genomic sequencing protocol that yields a positive display of 5-methylcytosine residues in individual DNA strands. Proc. Natl. Acad. Sci. USA 89: 1827–1831.
Garrigan, D., S. B. Kingan, A. J. Geneva, J. P. Vedanayagam, and D. C. Presgraves, 2014 Genome diversity and divergence in *Drosophila mauritiana*: multiple signatures of faster X evolution. Genome Biol. Evol. 6: 2444–2458.
Geraldes, A., P. Basset, B. Gibson, K. L. Smith, B. Harr *et al.*, 2008 Inferring the history of speciation in house mice from autosomal, X-linked, Y-linked and mitochondrial genes. Mol. Ecol. 17: 5349–5363.
Getun, I. V., B. Torres, and P. R. J. Bois, 2011 Flow cytometry purification of mouse meiotic cells. J. Vis. Exp. 50: e2602.
Gibson, G., and B. Weir, 2005 The quantitative genetics of transcription. Trends Genet. 21: 616–623.
Goncalves, A., S. Leigh-Brown, D. Thybert, K. Stefflova, E. Turro *et al.*, 2012 Extensive compensatory *cis-trans* regulation in the evolution of mouse gene expression. Genome Res. 22: 2376–2384.
Good, J. M., and M. W. Nachman, 2005 Rates of protein evolution are positively correlated with developmental timing of expression during mouse spermatogenesis. Mol. Biol. Evol. 22: 1044–1052.
Good, J. M., M. D. Dean, and M. W. Nachman, 2008 A complex genetic basis to X-linked hybrid male sterility between two species of house mice. Genetics 179: 2213–2228.
Good, J. M., T. Giger, M. D. Dean, and M. W. Nachman, 2010 Widespread over-expression of the X chromosome in sterile F1 hybrid mice. PLoS Genet. 6: e1001148.
Grath, S., and J. Parsch, 2012 Rate of amino acid substitution is influenced by the degree and conservation of male-biased transcription over 50 myr of *Drosophila* evolution. Genome Biol. Evol. 4: 346–359.
Graze, R. M., L. M. McIntyre, B. J. Main, M. L. Wayne, and S. V. Nuzhdin, 2009 Regulatory divergence in *Drosophila melanogaster* and *D. simulans*, a genomewide analysis of allele-specific expression. Genetics 183: 547–561.
Guerrero, R. F., A. L. Posto, L. C. Moyle, and M. W. Hahn, 2016 Genome-wide patterns of regulatory divergence revealed by introgression lines. Evolution 70: 696–706.
Haldane, J. B. S., 1922 Sex ratio and unisexual sterility in hybrid animals. J. Genet. 12: 101–109.
Halligan, D. L., F. Oliver, A. Eyre-Walker, B. Harr, and P. D. Keightley, 2010 Evidence for pervasive adaptive protein evolution in wild mice. PLoS Genet. 6: e1000825–e1000829.
Halligan, D. L., F. Oliver, J. Guthrie, K. C. Stemshorn, B. Harr *et al.*, 2011 Positive and negative selection in murine ultraconserved noncoding elements. Mol. Biol. Evol. 28: 2651–2660.
Halligan, D. L., A. Kousathanas, R. W. Ness, B. Harr, L. Eöry *et al.*, 2013 Contributions of protein-coding and regulatory change to adaptive molecular evolution in murid rodents. PLoS Genet. 9: e1003995.
Hernando-Herraez, I., H. Heyn, M. Fernandez-Callejo, E. Vidal, H. Fernandez-Bellon *et al.*, 2015 The interplay between DNA

methylation and sequence divergence in recent human evolution. Nucleic Acids Res. 43: 8204–8214.
Holt, J., S. Huang, L. McMillan, and W. Wang, 2013 Read annotation pipeline for high-throughput sequencing data. BCB 13: 605–612.
Hu, Y. C., and S. H. Namekawa, 2015 Functional significance of the sex chromosomes during spermatogenesis. Reproduction 149: R265–R277.
Huang, S., C.-Y. Kao, L. McMillan, and W. Wang, 2013 Transforming genomes using MOD files with applications. BCB 13: 595–604.
Huang, S., J. Holt, C.-Y. Kao, L. McMillan, and W. Wang, 2014 A novel multi-alignment pipeline for high-throughput sequencing data. Database 2014: bau057.
Hvilsom, C., Y. Qian, T. Bataillon, Y. Li, T. Mailund *et al.*, 2012 Extensive X-linked adaptive evolution in central chimpanzees. Proc. Natl. Acad. Sci. USA 109: 2054–2059.
Jablonka, E., and M. J. Lamb, 1991 Sex chromosomes and speciation. Proc. Biol. Sci. 243: 203–208.
Jaquiery, J., S. Stoeckel, C. Rispe, L. Mieuzet, F. Legeai *et al.*, 2012 Accelerated evolution of sex chromosomes in aphids, an X0 system. Mol. Biol. Evol. 29: 837–847.
Johnston, D. S., W. W. Wright, P. Dicandeloro, E. Wilson, G. S. Kopf *et al.*, 2008 Stage-specific gene expression is a fundamental characteristic of rat spermatogenic cells and Sertoli cells. Proc. Natl. Acad. Sci. USA 105: 8315–8320.
Kampstra, P., 2008 Beanplot: a boxplot alternative for visual comparison of distributions. J. Stat. Softw. 28: 1–9.
Kayserili, M. A., D. T. Gerrard, P. Tomancak, and A. T. Kalinka, 2012 An excess of gene expression divergence on the X chromosome in *Drosophila* embryos: implications for the faster-X hypothesis. PLoS Genet. 8: e1003200.
Keane, T. M., L. Goodstadt, P. Danecek, M. A. White, K. Wong *et al.*, 2011 Mouse genomic variation and its effect on phenotypes and gene regulation. Nature 477: 289–294.
Kessler, M. D., and M. D. Dean, 2014 Effective population size does not predict codon usage bias in mammals. Ecol. Evol. 4: 3887–3900.
Khaitovich, P., I. Hellmann, W. Enard, K. Nowick, M. Leinweber *et al.*, 2005a Parallel patterns of evolution in the genomes and transcriptomes of humans and chimpanzees. Science 309: 1850–1854.
Khaitovich, P., S. Pääbo, and G. Weiss, 2005b Toward a neutral evolutionary model of gene expression. Genetics 170: 929–939.
Khil, P. P., N. A. Smirnova, P. J. Romanienko, and R. D. Camerini-Otero, 2004 The mouse X chromosome is enriched for sex-biased genes not subject to selection by meiotic sex chromosome inactivation. Nat. Genet. 36: 642–646.
Kim, D., G. Pertea, C. Trapnell, H. Pimentel, R. Kelley *et al.*, 2013 TopHat2: accurate alignment of transcriptomes in the presence of insertions, deletions and gene fusions. Genome Biol. 14: R36.
King, M. C., and A. C. Wilson, 1975 Evolution at two levels in humans and chimpanzees. Science 188: 107–116.
Kohn, M., H. Kehrer-Sawatzki, W. Vogel, J. A. M. Graves, and H. Hameister, 2004 Wide genome comparisons reveal the origins of the human X chromosome. Trends Genet. 20: 598–603.
Kousathanas, A., D. L. Halligan, and P. D. Keightley, 2014 Faster-X adaptive protein evolution in house mice. Genetics 196: 1131–1143.
Landry, C. R., P. J. Wittkopp, C. H. Taubes, J. M. Ranz, A. G. Clark *et al.*, 2005 Compensatory *cis-trans* evolution and the dysregulation of gene expression in interspecific hybrids of *Drosophila*. Genetics 171: 1813–1822.
Langley, C. H., K. Stevens, C. Cardeno, Y. C. G. Lee, D. R. Schrider *et al.*, 2012 Genomic variation in natural populations of *Drosophila melanogaster*. Genetics 192: 533–598.
Lattin, J. E., K. Schroder, A. I. Su, J. R. Walker, J. Zhang *et al.*, 2008 Expression analysis of G Protein-Coupled Receptors in mouse macrophages. Immunome Res. 4: 5–13.
Lemos, B., C. D. Meiklejohn, M. Cáceres, and D. L. Hartl, 2004 Rates of divergence in gene expression profiles of primates, mice and flies: stabilizing selection and variability among functional categories. Evolution 59: 126–137.
Lemos, B., L. O. Araripe, P. Fontanillas, and D. L. Hartl, 2008 Dominance and the evolutionary accumulation of *cis*- and *trans*-effects on gene expression. Proc. Natl. Acad. Sci. USA 105: 14471–14476.
Li, E., T. H. Bestor, and R. Jaenisch, 1992 Targeted mutation of the DNA methyltransferase gene results in embryonic lethality. Cell 69: 915–926.
Li, H., and R. Durbin, 2009 Fast and accurate short read alignment with Burrows-Wheeler transform. Bioinformatics 25: 1754–1760.
Liao, B. Y., and J. Zhang, 2006 Low rates of expression profile divergence in highly expressed genes and tissue-specific genes during mammalian evolution. Mol. Biol. Evol. 23: 1119–1128.
Liao, B.-Y., N. M. Scott, and J. Zhang, 2006 Impacts of gene essentiality, expression pattern, and gene compactness on the evolutionary rate of mammalian proteins. Mol. Biol. Evol. 23: 2072–2080.
Lifschytz, E., and D. L. Lindsley, 1972 The role of X-chromosome inactivation during spermatogenesis. Proc. Natl. Acad. Sci. USA 69: 182–186.
Llopart, A., 2015 Parallel faster-X evolution of gene expression and protein sequences in *Drosophila*: beyond differences in expression properties and protein interactions. PLoS One 10: e0116829.
Lyon, M. F., 1961 Gene action in the X-chromosome of the mouse (*Mus musculus* L.). Nature 190: 372–373.
Lyon, M. F., 1962 Sex chromatin and gene action in the mammalian X-chromosome. Am. J. Hum. Genet. 14: 135–148.
Mack, K. L., P. Campbell, and M. W. Nachman, 2016 Gene regulation and speciation in house mice. Genome Res. 26: 451–461.
Mank, J. E., E. Axelsson, and H. Ellegren, 2007 Fast-X on the Z: rapid evolution of sex-linked genes in birds. Genome Res. 17: 618–624.
Mank, J. E., B. Vicoso, S. Berlin, and B. Charlesworth, 2010 Effective population size and the faster-X effect: empirical results and their interpretation. Evolution 64: 663–674.
McCarthy, D. J., Y. Chen, and G. K. Smyth, 2012 Differential expression analysis of multifactor RNA-Seq experiments with respect to biological variation. Nucleic Acids Res. 40: 4288–4297.
McKenna, A., M. Hanna, E. Banks, A. Sivachenko, K. Cibulskis *et al.*, 2010 The Genome Analysis Toolkit: a MapReduce framework for analyzing next-generation DNA sequencing data. Genome Res. 20: 1297–1303.
McManus, C. J., J. D. Coolon, M. O. Duff, J. Eipper-Mains, B. R. Graveley *et al.*, 2010 Regulatory divergence in *Drosophila* revealed by mRNA-seq. Genome Res. 20: 816–825.
Meiklejohn, C. D., E. L. Landeen, J. M. Cook, S. B. Kingan, and D. C. Presgraves, 2011 Sex chromosome-specific regulation in the *Drosophila* male germline but little evidence for chromosomal dosage compensation or meiotic inactivation. PLoS Biol. 9: e1001126.
Meiklejohn, C. D., J. D. Coolon, D. L. Hartl, and P. J. Wittkopp, 2014 The roles of *cis*- and *trans*-regulation in the evolution of regulatory incompatibilities and sexually dimorphic gene expression. Genome Res. 24: 84–95.
Meisel, R. P., 2011 Towards a more nuanced understanding of the relationship between sex-biased gene expression and rates of protein-coding sequence evolution. Mol. Biol. Evol. 28: 1893–1900.

Meisel, R. P., and T. Connallon, 2013 The faster-X effect: integrating theory and data. Trends Genet. 29: 537–544.
Meisel, R. P., J. H. Malone, and A. G. Clark, 2012a Faster-X evolution of gene expression in *Drosophila*. PLoS Genet. 8: e1003013.
Meisel, R. P., J. H. Malone, and A. G. Clark, 2012b Disentangling the relationship between sex-biased gene expression and X-linkage. Genome Res. 22: 1255–1265.
Meyer, M., and M. Kircher, 2010 Illumina sequencing library preparation for highly multiplexed target capture and sequencing. Cold Spring Harb. Protoc. 2010: t5448.
Miyata, T., H. Hayashida, K. Kuma, K. Mitsuyasu, and T. Yasunaga, 1987 Male-driven molecular evolution: a model and nucleotide sequence analysis. Cold Spring Harb. Symp. Quant. Biol. 52: 863–867.
Molaro, A., E. Hodges, F. Fang, Q. Song, W. R. McCombie *et al.*, 2011 Sperm methylation profiles reveal features of epigenetic inheritance and evolution in primates. Cell 146: 1029–1041.
Mueller, J. L., S. K. Mahadevaiah, P. J. Park, P. E. Warburton, D. C. Page *et al.*, 2008 The mouse X chromosome is enriched for multicopy testis genes showing postmeiotic expression. Nat. Genet. 40: 794–799.
Mueller, J. L., H. Skaletsky, L. G. Brown, S. Zaghlul, S. Rock *et al.*, 2013 Independent specialization of the human and mouse X chromosomes for the male germ line. Nat. Genet. 45: 1083–1087.
Nam, K., K. Munch, A. Hobolth, J. Y. Dutheil, and K. R. Veeramah *et al.*, 2015 Extreme selective sweeps independently targeted the X chromosomes of the great apes. Proc. Natl. Acad. Sci. USA 112: 6413–6418.
Namekawa, S. H., P. J. Park, L.-F. Zhang, J. E. Shima, J. R. McCarrey *et al.*, 2006 Postmeiotic sex chromatin in the male germline of mice. Curr. Biol. 16: 660–667.
Nguyen, L. P., N. Galtier, and B. Nabholz, 2015 Gene expression, chromosome heterogeneity and the fast-X effect in mammals. Biol. Lett. 11: 20150010.
Ohno, S., 1967 *Sex Chromosomes and Sex-Linked Genes*, Springer-Verlag, New York.
Okano, M., D. W. Bell, D. A. Haber, and E. Li, 1999 DNA methyltransferases Dnmt3a and Dnmt3b are essential for de novo methylation and mammalian development. Cell 99: 247–257.
Oksanen J., F. G. Blanchet, R. Kindt, P. Legendre, P. R. Minchin *et al.*, 2015 vegan: community ecology package. R package version 2.3–1.
Pages H., R. Gentleman, P. Aboyoun, and S. DebRoy, 2008 Biostrings: string objects representing biological sequences, and matching algorithms R package version 2.38.2.
Potrzebowski, L., N. Vinckenbosch, A. C. Marques, F. Chalmel, B. Jégou *et al.*, 2008 Chromosomal gene movements reflect the recent origin and biology of therian sex chromosomes. PLoS Biol. 6: e80.
R Development Core Team, 2014 R: A Language and Environment for Statistical Computing. R Foundation for Statistical Computing, Vienna.
Reik, W., 2007 Stability and flexibility of epigenetic gene regulation in mammalian development. Nature 447: 425–432.
Reik, W., W. Dean, and J. Walter, 2001 Epigenetic reprogramming in mammalian development. Science 293: 1089–1093.
Rice, W. R., 1984 Sex chromosomes and the evolution of sexual dimorphism. Evolution 38: 735–742.
Robinson, M. D., and A. Oshlack, 2010 A scaling normalization method for differential expression analysis of RNA-seq data. Genome Biol. 11: R25.
Robinson, M. D., D. J. McCarthy, and G. K. Smyth, 2010 edgeR: a Bioconductor package for differential expression analysis of digital gene expression data. Bioinformatics 26: 139–140.
Sackton, T. B., R. B. Corbett-Detig, J. Nagaraju, L. Vaishna, K. P. Arunkumar *et al.*, 2014 Positive selection drives faster-Z evolution in silkmoths. Evolution 68: 2331–2342.
Saglican, E., E. Ozkurt, H. Hu, B. Erdem, and P. Khaitovich, 2014 Heterochrony explains convergent testis evolution in primates. bioRxiv 010553, DOI: 10.1101/010553.
Scavetta, R. J., and D. Tautz, 2010 Copy number changes of CNV regions in intersubspecific crosses of the house mouse. Mol. Biol. Evol. 27: 1845–1856.
Schaefke, B., J. J. Emerson, T. Y. Wang, M. Y. J. Lu, L. C. Hsieh *et al.*, 2013 Inheritance of gene expression level and selective constraints on *trans*- and *cis*-regulatory changes in yeast. Mol. Biol. Evol. 30: 2121–2133.
Schultz, N., F. K. Hamra, and D. L. Garbers, 2003 A multitude of genes expressed solely in meiotic or postmeiotic spermatogenic cells offers a myriad of contraceptive targets. Proc. Natl. Acad. Sci. USA 100: 12201–12206.
Shen, S. Q., E. Turro, and J. C. Corbo, 2014 Hybrid mice reveal parent-of-origin and *cis*- and *trans*-regulatory effects in the retina. PLoS One 9: e109382.
Shi, X., D. W.-K. Ng, C. Zhang, L. Comai, W. Ye *et al.*, 2012 *Cis*- and *trans*-regulatory divergence between progenitor species determines gene-expression novelty in *Arabidopsis* allopolyploids. Nat. Commun. 3: 950–959.
Shima, J. E., D. J. McLean, J. R. McCarrey, and M. D. Griswold, 2004 The murine testicular transcriptome: characterizing gene expression in the testis during the progression of spermatogenesis. Biol. Reprod. 71: 319–330.
Sin, H. S., Y. Ichijima, E. Koh, M. Namiki, and S. H. Namekawa, 2012 Human postmeiotic sex chromatin and its impact on sex chromosome evolution. Genome Res. 22: 827–836.
Singh, N. D., J. C. Davis, and D. A. Petrov, 2005 X-linked genes evolve higher codon bias in *Drosophila* and *Caenorhabditis*. Genetics 171: 145–155.
Smedley, D., S. Haider, S. Durinck, L. Pandini, P. Provero *et al.*, 2015 The BioMart community portal: an innovative alternative to large, centralized data repositories. Nucleic Acids Res. 43: W598.
Smith, A. D., Z. Xuan, and M. Q. Zhang, 2008 Using quality scores and longer reads improves accuracy of Solexa read mapping. BMC Bioinformatics 9: 128.
Smith, A. D., W. Y. Chung, E. Hodges, J. Kendall, G. Hannon *et al.*, 2009 Updates to the RMAP short-read mapping software. Bioinformatics 25: 2841–2842.
Snyder, R. L., 1967 Fertility and reproductive performance of grouped male mice, pp. 458–472 in *Comparative Aspects of Reproductive Failure*, edited by K. Benirschke. Springer-Verlag, New York.
Song, Q., B. Decato, E. E. Hong, M. Zhou, F. Fang *et al.*, 2013 A reference methylome database and analysis pipeline to facilitate integrative and comparative epigenomics. PLoS One 8: e81148.
Stamatakis, A., 2014 RAxML version 8: a tool for phylogenetic analysis and post-analysis of large phylogenies. Bioinformatics 30: 1312–1313.
Su, A. I., M. P. Cooke, K. A. Ching, Y. Hakak, J. R. Walker *et al.*, 2002 Large-scale analysis of the human and mouse transcriptomes. Proc. Natl. Acad. Sci. USA 99: 4465–4470.
Torgerson, D. G., and R. S. Singh, 2003 Sex-linked mammalian sperm proteins evolve faster than autosomal ones. Mol. Biol. Evol. 20: 1705–1709.
Torgerson, D. G., and R. S. Singh, 2006 Enhanced adaptive evolution of sperm-expressed genes on the mammalian X chromosome. Heredity 96: 1–6.
Turner, J. M. A., 2007 Meiotic sex chromosome inactivation. Development 134: 1823–1831.
Turner, L. M., M. A. White, D. Tautz, and B. A. Payseur, 2014 Genomic networks of hybrid sterility. PLoS Genet. 10: e1004162.
Veeramah, K. R., R. N. Gutenkunst, A. E. Woerner, J. C. Watkins, and M. F. Hammer, 2014 Evidence for increased levels of positive and negative selection on the X chromosome *vs.* autosomes in humans. Mol. Biol. Evol. 31: 2267–2282.

Vibranovski, M. D., 2014 Meiotic sex chromosome inactivation in *Drosophila*. J Genomics 2: 104–117.
Vicoso, B., and B. Charlesworth, 2006 Evolution on the X chromosome: unusual patterns and processes. Nat. Rev. Genet. 7: 645–653.
Vicoso, B., and B. Charlesworth, 2009 Effective population size and the faster-X effect: an extended model. Evolution 63: 2413–2426.
Wang, P. J., J. R. McCarrey, F. Yang, and D. C. Page, 2001 An abundance of X-linked genes expressed in spermatogonia. Nat. Genet. 27: 422–426.
Wang, Z., M. Gerstein, and M. Snyder, 2009 RNA-Seq: a revolutionary tool for transcriptomics. Nat. Rev. Genet. 10: 57–63.
Warnes G. R., B. Bolker, L. Bonebakker, R. Gentleman, W. Huber *et al.*, 2015 gplots: various R programming tools for plotting data. R package version 2.17.
Wittkopp, P. J., B. K. Haerum, and A. G. Clark, 2004 Evolutionary changes in *cis* and *trans* gene regulation. Nature 430: 85–88.
Wittkopp, P. J., B. K. Haerum, and A. G. Clark, 2008 Regulatory changes underlying expression differences within and between *Drosophila* species. Nat. Genet. 40: 346–350.
Wright, A. E., P. W. Harrison, F. Zimmer, S. H. Montgomery, M. A. Pointer *et al.*, 2015 Variation in promiscuity and sexual selection drives avian rate of Faster-Z evolution. Mol. Ecol. 24: 1218–1235.
Wu, C.-I., and A. W. Davis, 1993 Evolution of postmating reproductive isolation: the composite nature of Haldane's rule and its genetic bases. Am. Nat. 142: 187–212.
Yanai, I., H. Benjamin, M. Shmoish, V. Chalifa-Caspi, M. Shklar *et al.*, 2005 Genome-wide midrange transcription profiles reveal expression level relationships in human tissue specification. Bioinformatics 21: 650–659.
Yang, H., J. R. Wang, J. P. Didion, R. J. Buus, T. A. Bell *et al.*, 2011 Subspecific origin and haplotype diversity in the laboratory mouse. Nat. Genet. 43: 648–655.
Yang, Z., 2007 PAML 4: phylogenetic analysis by maximum likelihood. Mol. Biol. Evol. 24: 1586–1591.
Zhang, Y. E., M. D. Vibranovski, P. Landback, G. A. B. Marais, and M. Long, 2010 Chromosomal redistribution of male-biased genes in mammalian evolution with two bursts of gene gain on the X chromosome. PLoS Biol. 8: 2527.

Communicating editor: B. A. Payseur

GENETICS

Supporting Information
www.genetics.org/lookup/suppl/doi:10.1534/genetics.116.186825/-/DC1

Contrasting Levels of Molecular Evolution on the Mouse X Chromosome

Erica L. Larson, Dan Vanderpool, Sara Keeble, Meng Zhou, Brice A. J. Sarver, Andrew D. Smith, Matthew D. Dean, and Jeffrey M. Good

DOI: 10.1534/genetics.116.186825

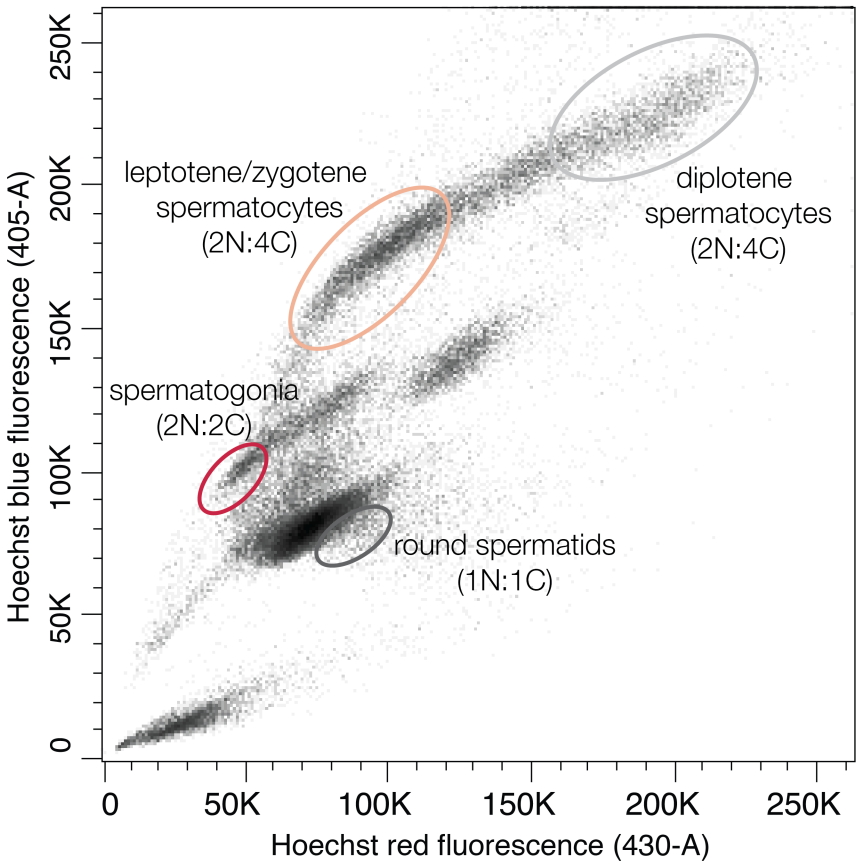

Figure S1. Florescence activated cell sorting of spermatogenic cell populations.
Representative profile of testis cells from a fertile mouse (M. m. musculus). Cells were isolated from four distinct populations: 1) spermatogonia (red), 2) leptotene/zygotene spermatocytes (orange), 3) diplotene spermatocytes (light gray) and 4) round spermatids (dark gray) using FACS. Dead cells stained with propidium idodide were excited at 488 nm and detected with 585/42 bandpass filter. Live cells stained with Hoechst were excited at 405 nm and detected with 450/40 (blue-shifted) and 610/20 (red-shifted) bandpass filters.

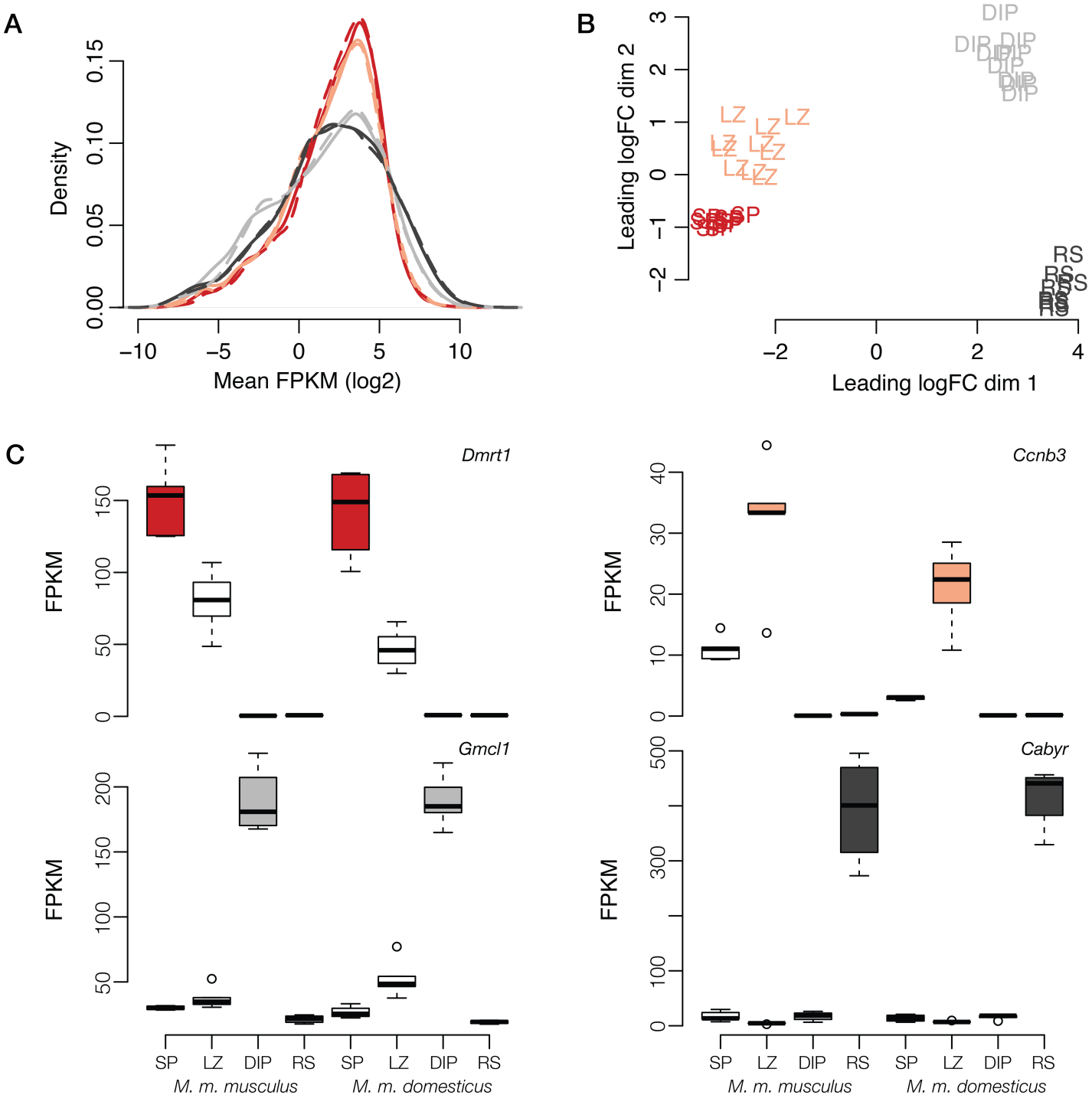

Figure S2. Purity of FACS spermatogenic cell populations.
(A) Relative expression level for each cell type: spermatogonia (red), leptotene/zygotene spermatocytes (orange), diplotene spermatocytes (light gray), and round spermatids (dark gray). Solid lines indicate expression in M. m. musculus and dashed lines M. m. domesticus. Each cell stage has a distinct expression profiles that are largely congruent between the two species. (B) Multidimensional scaling plot of distances between gene expression profiles. The distances on the plot represent the log2 fold changes between samples for genes that distinguish each cell type (i.e. genes with the largest logFC changes among cell types, or leading log-fold change). Distances are calculated as the root-mean-square deviation (Euclidean distance). SP = spermatogonia, LZ = leptotene/zygotene spermatocytes, DIP = diplotene spermatocytes, RS = round spermatids. (C) Boxplots of gene expression (FPKM) for four autosomal genes that have been previously documented to be highly expressed in one of the four targeted cell populations: Dmrt1: spermatogonia (Raymond et al. 2000); Ccnb3: leptotene/zygotene spermatocytes (Nguyen et al. 2002); Gmcl1: diplotene spermatocytes (Maekawa et al. 2004); Cabyr: round spermatids (Li et al. 2007).

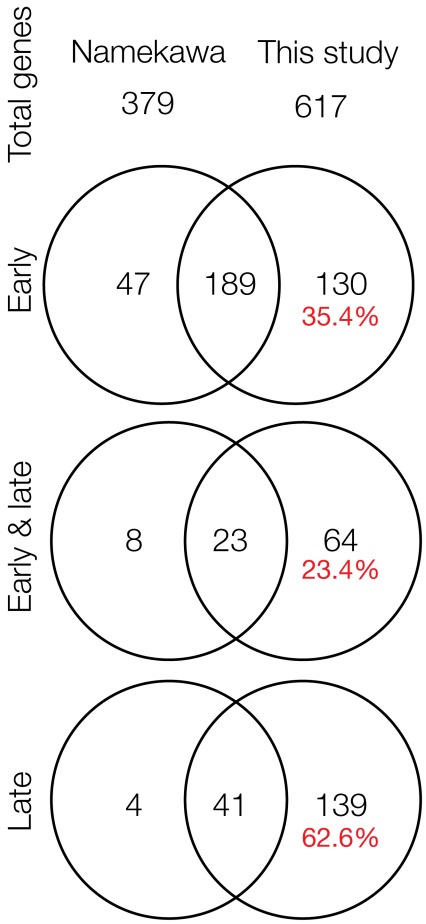

Figure S3. Stage-specific gene expression patterns on the X chromosome. Venn diagrams indicate the gene-by-gene correspondence with Namekawa et al. (2006) at three stages of spermatogenesis relative to MSCI. Many of these differences are multicopy/ampliconic genes (percent in red), which were not evaluated in Namekawa et al. (2006).

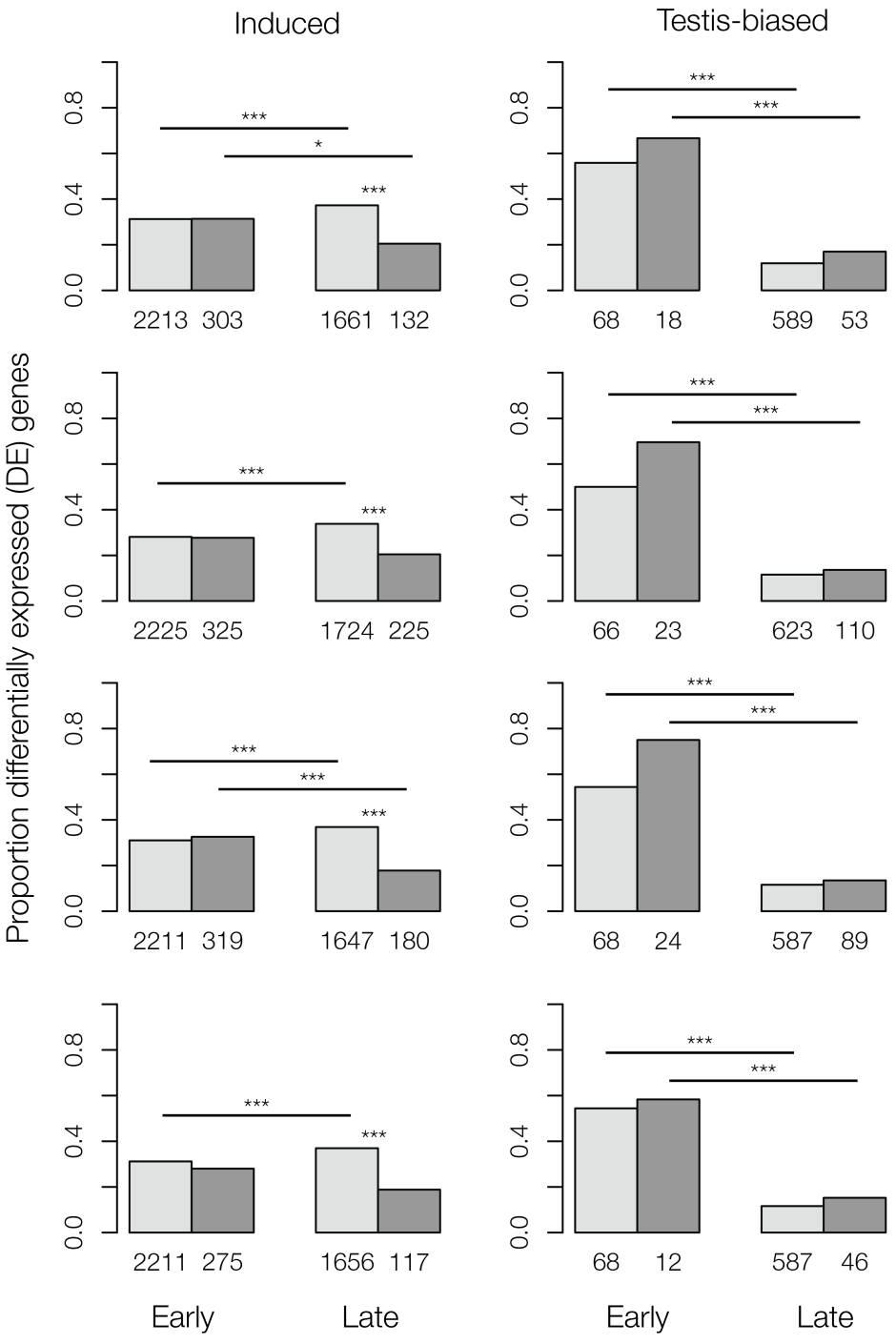

Figure S4. Comparisons of gene expression divergence between subspecies of M. musculus evaluated using different methods of handling multicopy/ampliconic X-linked genes. Bars represent the proportion of DE genes induced early and late in spermatogenesis on the autosomes (light gray) and the X chromosome (dark gray). The total number of genes in each category is listed below. We compared the proportion of DE genes between 1) the autosomes and the X chromosome and 2) between genes induced early and late in spermatogenesis. No matter how multicopy/ampliconic genes are evaluated there is slower-X chromosome expression divergence late in spermatogenesis. The autosomes have higher gene expression divergence late in spermatogenesis, compared to early. For both the autosomes and the X chromosome there were fewer testis-biased genes differentially expressed late in spermatogenesis. Significant differences in the proportion of DE genes (X2) are indicated for each contrast. FDR corrected P-values : * ≤ 0.05, ** ≤ 0.01, *** ≤ 0.001.

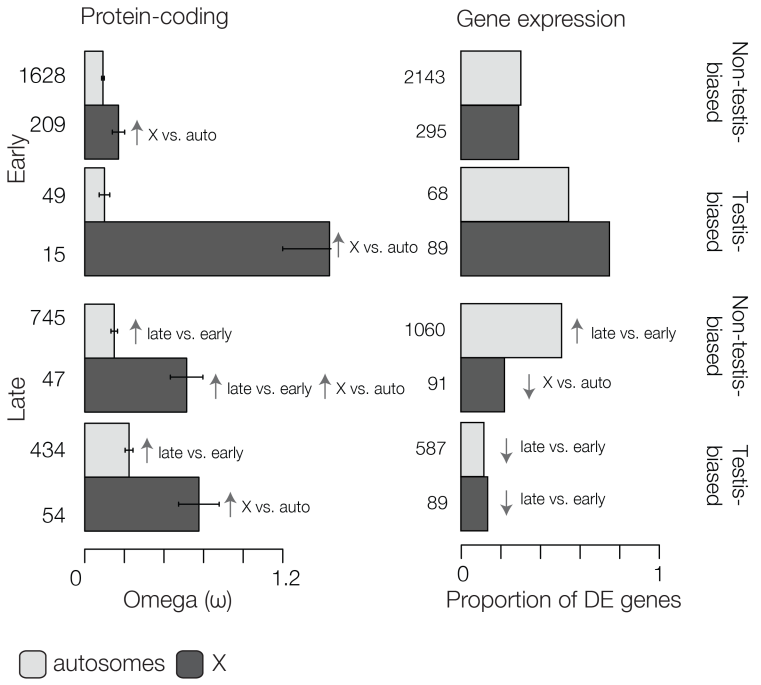

Figure S5. Evolutionary divergence in protein-coding sequence and expression level for testis-biased and non-testis-biased genes. (A) Median (± SE) estimates of protein-coding divergence (ω) among subspecies of M. musculus and M. spretus is higher for genes expressed late and for X-linked genes. (B) The proportion of differentially expressed (DE) genes between the subspecies of M. musculus. The evolution of X-linked genes is either equivalent or slower than autosomal genes and there is a marked drop in the proportion of DE genes for testis-biased genes expressed late in spermatogenesis. N = total number of genes. Significant differences in ω (Wilcoxon test) and proportion of DE genes (X2) are indicated for each contrast. FDR corrected P-values : * ≤ 0.05, ** ≤ 0.01, *** ≤ 0.001.

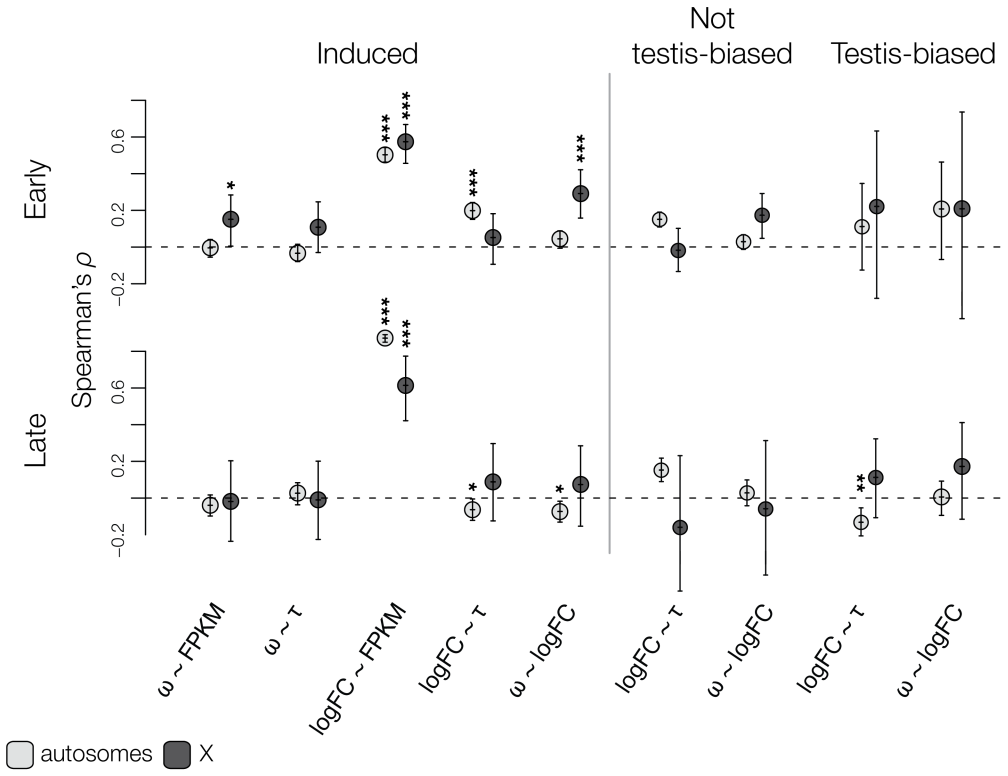

Figure S6. Correlations between protein-coding divergence and gene expression for genes induced early and late in spermatogenesis. Correlations between protein divergence (ω), expression level (normalized FPKM), tissue specificity (τ) and change in expression (logFC). Correlations were estimated using Spearman's ρ with confidence intervals estimated by bootstrapping the data 1,000 times. We considered ρ values significant when 95% confidence intervals did not overlap with zero and we estimated p-values using an asymptotic t approximation (as described in R package "cor.test"); in all cases significance determined by the two methods corresponded.

Table S1. Summary of RNA sequencing. Totals refer to the number of paired or unpaired reads at each step of the data analysis. Assigned reads are the number of reads that were assigned to a protein-coding gene (GRCm38, Ensembl release 78). Final library sizes are the genes retained after filtering for protein-coding genes expressed at FPKM > 1 in a minimum of 4 samples. Multiply-mapped reads were only included in the final libraries for X-linked multicopy/ampliconic genes and Y-linked genes. Totals for each subspecies by cell type are in bold.

	Mouse	Age	Cell	Reads	Trimmed reads	Mapped reads	Assigned reads	Single mapping final library	Multiple mapping final library
M. m. musculus (CZECHII x PWK)	CCPP21-1	65	SP	15875714	14848677	13127558	9834225	9343742	9438023
			LZ	38586917	37032474	33729358	25671640	24636552	24836457
			DIP	35739517	34497256	31703960	24293673	23292621	23301083
			RS	34596233	33382086	30664569	24243491	23300957	23414883
	CCPP21-2	76	SP	39606549	37871137	34178950	26241291	25136807	25498493
			LZ	13274948	12559289	11368859	8659209	8264666	8299704
			DIP	39629739	38139261	34959747	26764307	25619384	25629957
			RS	11117634	10666428	9853080	7818929	7491314	7511231
	CCPP21-3	62	SP	10875913	10336701	9178487	7007838	6693973	6786489
			LZ	10214496	9615769	8645697	6649903	6374380	6429624
			DIP	11234392	10680478	9749822	7618069	7299566	7300413
			RS	36015123	34438340	31514963	25215833	24221070	24327358
	CCPP23-2	88	SP	22470810	21173075	19203097	14903162	14253664	14510980
			LZ	20124143	19430801	17606223	13374428	12805427	12937534
	CCPP27-3	73	SP	27652764	26747191	24697801	19293162	18507090	18761104

			LZ	25904910	25031211	23015951	17486007	16737618	16864374
			DIP	23946157	23183181	21574369	16468263	15753679	15756065
			RS	23017070	22275222	20709463	16429439	15773238	15862479
	Total *M. m. musculus*		**SP**	**116481750**	**110976781**	**100385893**	**77279678**	**73935276**	**74995089**
			LZ	**108105414**	**103669544**	**94366088**	**71841187**	**68818643**	**69367693**
			DIP	**110549805**	**106500176**	**97987898**	**75144312**	**71965250**	**71987518**
			RS	**104746060**	**100762076**	**92742075**	**73707692**	**70786579**	**71115951**
M. m. domesticus (WSB x LEWES)	WWLL3-1	64	SP	10552073	9978631	8795436	6396396	6034274	6068526
			LZ	17496084	16453925	14983762	10935894	10487355	10527944
			DIP	10985159	10465262	9717157	7421723	7082080	7083212
			RS	28470583	27324185	25057853	19754120	18897980	18992725
	WWLL4-1	61	LZ	10037623	9498288	8748569	6548674	6276922	6297187
			DIP	21718977	21185220	19655034	14947210	14313697	14318678
	WWLL6-1	68	SP	22781845	21807076	20053041	15009740	14380183	14519384
			DIP	21015043	20294090	18663797	14166523	13567330	13571654
			RS	10194381	9567846	8727864	6934032	6634627	6651521
	WWLL7-1	83	DIP	9987292	9407914	8665965	6685306	6386318	6387575
	WWLL7-2	87	SP	12926098	12176326	11147407	8182360	7796175	7861099
			LZ	10043616	9604294	8958383	6611216	6310834	6337166
			DIP	35009424	33815532	31378539	23477459	22459116	22463505

		RS	32787873	31618688	29303014	23688278	22697765	22819157
WWLL7-3	89	SP	41141115	39118684	35755121	26425725	25189148	25420696
		LZ	42701434	40933370	37863206	27603407	26431445	26565582
WWLL13-1	70	LZ	22280208	21693473	19745862	14644284	13988194	14016647
		RS	18755440	18268381	16871281	13783211	13235943	13327211
Total *M. m. domesticus*		**SP**	**87401131**	**83080717**	**75751005**	**56014221**	**53399780**	**53869705**
		LZ	**102558965**	**98183350**	**90299782**	**66343475**	**63494750**	**63744526**
		DIP	**98715895**	**95168018**	**88080492**	**66698221**	**63808541**	**63824624**
		RS	**90208277**	**86779100**	**79960012**	**64159641**	**61466315**	**61790614**

Table S2. Substitution rates across different evolutionary contrasts. Estimates of median (± standard error) ω, nonsynonymous substitution rates (dN) and synonymous substitution rates (dS) among *M. m. musculus*, *M. m. domesticus* and *M. spretus* and *Rattus norvegicus*. Significant differences (Wilcoxon test) between the autosomes and X chromosome are indicated by FDR corrected (Benjamini and Hochberg 1995) *P*-values: ** < 0.01, *** < 0.001. **A)** Genes expressed in spermatogenesis. **B)** Genes induced early in spermatogenesis. **C)** Genes expressed late in spermatogenesis. Bold values indicate significant differences among early and late genes.

A	**All Genes**	*M. m. domesticus* vs *M. m. musculus*		*M. m. domesticus* vs. *M. spretus*		*M. m. musculus* vs. *M. spretus*		*M. m. domesticus* vs. *R. norvegicus*	
N	Auto	9,898		9,898		9,898		10,565	
	X	417		417		417		311	
ω	Auto	0.091	± 2.29×10^{-1}	0.110	± 7.75×10^{-2}	0.110	± 7.85×10^{-2}	0.119	± 1.61×10^{-3}
	X	0.188^{***}	± 1.73	0.251^{***}	± 7.05×10^{-1}	0.218^{***}	± 5.78×10^{-1}	0.192^{***}	± 1.33×10^{-2}
dN	Auto	0.001	± 2.43×10^{-5}	0.002	± 4.60×10^{-5}	0.002	± 4.68×10^{-5}	0.023	± 3.38×10^{-4}
	X	0.001^{**}	± 1.50×10^{-4}	0.003^{***}	± 4.25×10^{-4}	0.003^{***}	± 4.44×10^{-4}	0.029^{***}	± 2.82×10^{-3}
dS	Auto	0.008	± 7.21×10^{-5}	0.019	± 9.79×10^{-5}	0.019	± 9.74×10^{-5}	0.196	± 5.73×10^{-4}
	X	0.004^{***}	± 2.90×10^{-4}	0.014^{***}	± 4.51×10^{-4}	0.015^{***}	± 4.66×10^{-4}	0.156^{***}	± 3.52×10^{-3}
	dS^X/dS^{auto}	0.572		0.740		0.796		0.796	
B	**Early**								
N	Auto	1,677		1,677		1,677		1,800	
	X	224		224		224		181	
ω	Auto	0.064	± 5.20×10^{-1}	0.091	± 1.88×10^{-1}	0.089	± 2.27×10^{-1}	0.100	± 3.31×10^{-3}
	X	0.146^{***}	± 2.12	0.184^{***}	± 7.60×10^{-1}	0.166^{***}	± 6.22×10^{-1}	0.178^{***}	± 1.70×10^{-2}
dN	Auto	< 0.001	± 5.26×10^{-5}	0.002	± 1.00×10^{-4}	0.002	± 9.65×10^{-5}	0.019	± 6.68×10^{-4}
	X	0.001	± 2.00×10^{-4}	0.002^{**}	± 5.23×10^{-4}	0.002^{**}	± 5.72×10^{-4}	0.024^{***}	± 3.44×10^{-3}
dS	Auto	0.008	± 1.80×10^{-4}	0.020	± 2.43×10^{-4}	0.020	± 2.42×10^{-4}	0.199	± 1.38×10^{-3}
	X	0.004^{***}	± 3.94×10^{-4}	0.014^{***}	± 5.89×10^{-4}	0.014^{***}	± 5.97×10^{-4}	0.154^{***}	± 4.61×10^{-3}
	dS^X/dS^{auto}	0.482		0.686		0.730		0.774	
C	**Late**								
N	Auto	1,179		1,179		1,179		1,188	
	X	102		102		102		52	
ω	Auto	**0.159**	± 7.55×10^{-1}	**0.169**	± 2.51×10^{-1}	**0.179**	± 2.51×10^{-1}	**0.190**	± 6.93×10^{-3}
	X	$\mathbf{0.565}^{***}$	± 4.46	$\mathbf{0.528}^{***}$	± 1.67	$\mathbf{0.454}^{***}$	± 1.67	$\mathbf{0.353}^{***}$	± 3.85×10^{-2}
dN	Auto	**0.001**	± 1.14×10^{-4}	**0.004**	± 1.96×10^{-4}	**0.004**	± 2.05×10^{-4}	**0.037**	± 1.44×10^{-3}
	X	$\mathbf{0.002}^{***}$	± 3.68×10^{-4}	$\mathbf{0.009}^{***}$	± 1.09×10^{-3}	$\mathbf{0.009}^{***}$	± 1.08×10^{-3}	$\mathbf{0.068}^{***}$	± 8.61×10^{-3}
dS	Auto	0.008	± 2.22×10^{-4}	**0.021**	± 2.81×10^{-4}	**0.022**	± 2.81×10^{-4}	0.202	± 1.67×10^{-3}
	X	0.005^{***}	± 6.45×10^{-4}	$\mathbf{0.017}^{***}$	± 1.06×10^{-3}	$\mathbf{0.018}^{**}$	± 1.11×10^{-3}	**0.201**	± 8.98×10^{-3}
	dS^X/dS^{auto}	0.554		0.821		0.839		0.995	

Table S3. Protein-coding divergence estimated with global rates tested at different expression thresholds and read count handling.

A. Genes induced early and late in spermatogenesis

		N		d_N		d_S		ω	
		Auto	X	Auto	X	Auto	X	Auto	X
FPKM >1	early	1677	224	0.002 (±1.18x10^{-4})	0.003 (±6.30x10^{-4})[1]	0.025 (±2.72x10^{-4})	0.016 (±6.62x10^{-4}) [1]	0.092 (±6.35x10^{-3})	0.183 (±3.61x10^{-2}) [1]
	late	1179	101	0.004 (±2.45x10^{-4}) [2]	0.010 (±1.22x10^{-3}) [1, 2]	0.026 (±3.16x10^{-4}) [2]	0.021 (±1.00x10^{-3}) [1, 2]	0.177 (±1.27x10^{-2}) [2]	0.535 (±6.68x10^{-2}) [1, 2]
FPKM >5	early	1145	138	0.002 (±1.40x10^{-4})	0.003 (±9.27x10^{-4}) [1]	0.024 (±3.33x10^{-4})	0.017 (±9.03x10^{-4}) [1]	0.086 (±7.96x10^{-3})	0.193 (±5.26x10^{-2}) [1]
	late	780	91	0.005 (±2.68x10^{-4}) [2]	0.012 (±1.32x10^{-3}) [1, 2]	0.025 (±3.86x10^{-4})	0.021 (±1.09x10^{-3}) [1,2]	0.197 (±1.65x10^{-2}) [2]	0.584 (±7.28x10^{-2}) [1, 2]
FPKM >10	early	891	98	0.002 (±1.37x10^{-4})	0.004 (±1.22x10^{-3}) [1]	0.023 (±3.81x10^{-4})	0.017 (±1.07x10^{-3}) [1]	0.084 (±7.66x10^{-3})	0.283 (±6.42x10^{-2}) [1]
	late	613	75	0.005 (±2.40x10^{-4}) [2]	0.012 (±1.53x10^{-3}) [1, 2]	0.025 (±4.24x10^{-4}) [2]	0.022 (±1.25x10^{-3}) [2]	0.198 (±1.61x10^{-2}) [2]	0.584 (±8.38x10^{-2}) [1, 2]
Single-mapped Paralogs removed	early	1678	216	0.002 (±1.17x10^{-4})	0.003 (±6.18x10^{-4})[1]	0.025 (±2.72x10^{-4})	0.016 (±6.73x10^{-4}) [1]	0.093 (±6.35x10^{-3})	0.173 (±3.23x10^{-2}) [1]
	late	1190	84	0.004 (±2.43x10^{-4}) [2]	0.009 (±1.37x10^{-3}) [1,2]	0.026 (±3.15x10^{-4}) [2]	0.020 (±9.78x10^{-4}) [1, 2]	0.177 (±1.26x10^{-2}) [2]	0.532 (±7.70x10^{-2}) [1,2]
	early	1677	203	0.002 (±1.18x10^{-4})	0.003 (±4.69x10^{-4})	0.025 (±2.72x10^{-4})	0.016 (±6.71x10^{-4}) [1]	0.092 (±6.35x10^{-3})	0.157 (±3.30x10^{-2}) [1]
	late	1187	73	0.004 (±2.44x10^{-4}) [2]	0.009 (±1.49x10^{-3}) [1,2]	0.026 (±3.15x10^{-4}) [2]	0.020 (±1.02x10^{-3}) [1,2]	0.177 (±1.27x10^{-2}) [2]	0.529 (±8.44x10^{-2}) [1,2]

B. Testis-biased genes

FPKM >1	early	49	15	0.003 (±6.57x10^{-4})	0.035 (±4.97x10^{-3})[1]	0.023 (±1.48x10^{-3})	0.021 (±2.76x10^{-3})	0.100 (±2.67x10^{-2})	1.236 (±2.37x10^{-1}) [1]
	late	434	54	0.005 (±3.79x10^{-4}) [2]	0.013 (±1.98x10^{-3}) [1]	0.024 (±5.07x10^{-4})	0.022 (±1.46x10^{-3})	0.224 (±1.99x10^{-2}) [2]	0.576 (±1.02x10^{-1}) [1]
FPKM >5	early	30	12	0.003 (±7.37x10^{-4})	0.036 (±5.63x10^{-3}) [1]	0.022 (±2.04x10^{-3})	0.028 (±3.30x10^{-3})	0.105 (±3.52x10^{-2})	1.261 (±2.51x10^{-1}) [1]
	late	417	54	0.005 (±3.43x10^{-4}) [2]	0.013 (±1.98x10^{-3}) [1]	0.024 (±5.10x10^{-4})	0.022 (±1.49x10^{-3})	0.224 (±1.97x10^{-2}) [2]	0.576 (±1.02x10^{-1}) [1]
FPKM >10	early	26	11	0.002 (±6.18x10^{-4})	0.037 (±6.11x10^{-3}) [1]	0.022 (±2.14x10^{-3})	0.029 (±3.10x10^{-3})	0.092 (±3.97x10^{-2})	1.236 (±2.01x10^{-1}) [1]
	late	382	48	0.005 (±2.84x10^{-4}) [2]	0.014 (±2.17x10^{-3}) [1]	0.024 (±5.28x10^{-4})	0.022 (±1.59x10^{-3})	0.222 (±1.80x10^{-2}) [2]	0.576 (±1.11x10^{-1}) [1]

[1] values are significantly different on the X chromosome
[2] different between early and late cell types

Table S4. **Slower-X and slower-late gene expression divergence.** Values represent the proportion of expressed genes that are DE for a given expression threshold. There is slower-X expression evolution for genes expressed or induced late in spermatogenesis using either absolute (by cell type) or relative (by stage) expression thresholds. Testis-biased genes have slower expression evolution late in spermatogenesis for both autosomal and X-linked genes. Enrichment of X-linked DE genes are based on chromosome-wise hypergeometric tests, FDR corrected *P*-values: *** ≤ 0.001.

		Expressed[1]		**Induced**[2]		**Testis-biased**[3]	
		Auto	X	Auto	X	Auto	X
By cell	Spermatogonia	0.24	0.29	0.28	0.30	0.25	**0.47*** **
	Leptotene/zygotene spermatocytes	0.37	0.37	0.42	**0.35***	0.49	0.67
	[6]Diplotene spermatocytes	0.34	**0.10*** **	0.32	**0.06*** **	0.18	0.05
	Round spermatids	0.41	**0.21*** **	0.34	**0.19*** **	0.18	0.15
By stage	Early	NA	NA	0.31	0.33	0.54	0.75
	Late	NA	NA	0.37	**0.18*** **	0.12	0.13

[1] Expressed = genes with FPKM > 1 in a minimum of 4 individuals for a given cell type (14,223 genes)
[2] % Induced = By cell: genes with a median FPKM > 2× the median FPKM of all other cell types combined out of the total genes expressed. By stage: genes with a maximum FPKM > 4× the maximum FPKM of all other stages combined. (Note: a gene can be induced in more than one cell type, but can only be induced at a single stage).
[3] Testis-biased = genes with higher expression in the testes compared 96 other tissues from the Mouse MOE430 Gene Atlas out of the total genes induced

Table S5. Expression divergence tested at different expression thresholds and read count handling.

		Genes induced early and late in spermatogenesis						Testis-biased genes					
		N		DE genes		Proportion DE		N		DE genes		Proportion DE	
		Auto	X	Auto	X	Auto	X	Auto	X	Auto	X	Auto	X
FPKM >1	early	2211	319	686	104	0.31	0.326	68	24	37	18	0.544	0.75
	late	1647	180	607	32	0.369[2]	0.178[1, 2]	587	89	68	12	0.116[2]	0.135[2]
FPKM >5	early	1487	201	290	43	0.195	0.214	43	18	17	9	0.395	0.5
	late	1068	158	218	18	0.204	0.114[1,2]	552	86	42	10	0.076[2]	0.116[2]
FPKM >10	early	1158	146	178	29	0.154	0.199	33	17	12	7	0.364	0.412
	late	841	128	92	11	0.109[2]	0.086[2]	506	77	26	8	0.051[2]	0.104[2]
Single-mapped	early	2213	303	692	95	0.313	0.314	68	18	38	12	0.559	0.667
	late	1661	132	619	27	0.373[2]	0.205[1,2]	589	53	70	9	0.119[2]	0.17[2]
Paralogs excluded	early	2211	275	689	77	0.312	0.28	68	12	37	7	0.544	0.583
	late	1656	117	612	22	0.37[2]	0.188[1]	587	46	68	7	0.116[2]	0.152[2]

[1] values are significantly different on the X chromosome
[2] different between early and late cell types

Table S6. Summary of methylome sequencing.

		M. m. musculus				*M. spretus*			
		MBS	MBS	MPB	MPB	SFM	SFM	STF	STF
Reads	**Sequenced reads**	133,333,334	117,743,000	133,333,334	113,114,760	124,649,806	123,778,534	113,303,048	113,114,760
	Distinctively mapped reads	96,034,500	84,382,644	95,597,173	85,213,907	94,176,379	92,085,631	84,504,104	85,099,535
	Average mismatch	1.6	1.6	1.6	1.5	1.2	1.2	1.4	1.4
	Number of effective reads[1]	63,134,279	54,263,768	62,528,427	54,036,091	66,877,509	62,314,211	57,404,575	57,639,591
	Number of fragments	37,644,198	32,453,755	36,938,190	30,766,347	37,947,447	36,219,474	33,044,671	32,409,608
	Median fragment size	231	231	233	226	244	227	232	245
Methylome	**BS conversion rate**	0.99	0.99	0.99	0.99	0.99	0.99	0.99	0.99
	Mutated CpGs	2,105,456	-	-	-	1,284,464	-	-	-
	CpGs covered[2]	78.1%	76.7%	78.0%	76.5%	79.1%	78.4%	75.9%	75.5%
	Average coverage for CpG sites	3.42	2.89	3.40	2.95	3.46	3.17	2.85	2.77
	Whole genome average	0.74	0.76	0.74	0.74	0.76	0.76	0.76	0.76
	Promoter average[3]	0.59	0.60	0.59	0.59	0.60	0.60	0.60	0.59

[1] Effective read means the read covers at least one CpG site.
[2] CpGs are considered after removing possible mutations. The total number of CpG sites after removing mutation is 19,762,381 for mm10, and 19,619,286 for ms10.
[3] Promoter is +/- 1kb around ENSEMBL gene TSS after collapsing overlapping regions. Promoter average methylation is calculated by taking average of mean methylations of all ENSEMBL promoters after collapsing and removing non-covered ones.

Table S7. Summary of properties of HMRs.

		Genome-wide					At promoters*				
	Methylome	**HMRs**	**Total bases**	**Mean size**	**Median size**	**Mean CpGs**	**HMRs**	**Total bases**	**Mean size**	**Median size**	**Mean CpGs**
Individual	MBS1	56,241	86,798,081	1543.3	1274	41.8	18,532	39,441,110	2128.3	1906	79.7
	MBS2	54,755	80,985,366	1479.0	1217	40.7	18,340	37,203,258	2028.5	1832.5	76.5
	MPB1	52,637	81,406,923	1546.6	1253	42.5	18,155	37,767,021	2080.3	1853	80.6
	MPB2	49,723	77,154,519	1551.7	1264	42.1	17,827	37,143,757	2083.6	1859	77.2
	SFM1	56,444	81,824,448	1449.7	1210	41.6	18,189	38,312,861	2106.4	1885	81.6
	SFM2	56,642	82,396,125	1454.7	1221	41.0	18,232	38,845,876	2130.6	1915.5	80.0
	STF1	52,494	77,289,689	1472.4	1229	41.2	17,963	37,683,287	2097.8	1898	77.8
	STF2	52,353	75,473,820	1441.6	1203	40.1	18,045	37,463,283	2076.1	1881	74.9
Pooled	MBS	60,365	88,214,987	1456.6	1190	41.6	18,751	38,569,986	2057.0	1859	84.0
	MPB	56,218	84,017,899	1494.5	1207	42.6	18,296	37,632,168	2056.9	1830	85.0
	SFM	62,414	85,364,437	1367.7	1137	40.8	18,540	38,633,309	2083.8	1879	85.9
	STF	58,242	77,266,636	1326.6	1099	40.6	18,328	36,943,101	2015.7	1837	83.4
	Musculus	62,455	88,839,792	1422.5	1144	41.2	15,693	34,955,661	2227.0	2000	96.0
	Spretus	66,112	86,855,708	1313.8	1083	39.9	18,732	38,632,217	2062.4	1873	87.7

*: Promoter is +/- 1kb around ENSEMBL gene TSS after collapsing overlapping regions.

Table S8. Correlations between methylation at promoters for different methylomes. Correlations are based on average promoter methylation. Approximately 33k ENSEMBLE promoters were selected as including at least 10 CpG sites and 30 mapped reads.

	MBS1	MBS2	MPB1	MPB2	SFM1	SFM2	STF1	STF2
MBS1	NA	0.703	0.666	0.650	0.609	0.602	0.581	0.575
MBS2	0.703	NA	0.656	0.642	0.601	0.595	0.574	0.568
MPB1	0.666	0.656	NA	0.698	0.605	0.598	0.580	0.573
MPB2	0.650	0.642	0.698	NA	0.592	0.585	0.567	0.562
SFM1	0.609	0.601	0.605	0.592	NA	0.753	0.668	0.661
SFM2	0.602	0.595	0.598	0.585	0.753	NA	0.662	0.655
STF1	0.581	0.574	0.580	0.567	0.668	0.662	NA	0.715
STF2	0.575	0.568	0.573	0.562	0.661	0.655	0.715	NA

Table S9. Summary of the observed and expected numbers of DMRs. Expectations are based on the proportion of CpG sites on each chromosome multiplied by the total number of DMRs.

	Chr	DMR 5 observed	CpG 7				Genome length			
				expected proportion	expected DMR 5	obs vs exp		expected proportion	expected DMR 5	obs vs exp
down-sampled	1	494	620661	0.06	596.47	0.83	195471971	0.07	711.00	0.69
	2	570	724025	0.07	695.80	0.82	182113224	0.07	662.41	0.86
	3	637	536890	0.05	515.96	1.23	160039680	0.06	582.12	1.09
	4	554	632991	0.06	608.32	0.91	156508116	0.06	569.28	0.97
	5	774	656520	0.07	630.93	1.23	151834684	0.06	552.28	1.40
	6	512	541635	0.05	520.52	0.98	149736546	0.06	544.65	0.94
	7	438	569974	0.06	547.76	0.80	145441459	0.06	529.02	0.83
	8	594	565361	0.06	543.32	1.09	129401213	0.05	470.68	1.26
	9	437	534742	0.05	513.90	0.85	124595110	0.05	453.20	0.96
	10	787	529774	0.05	509.12	1.55	130694993	0.05	475.39	1.66
	11	452	613752	0.06	589.83	0.77	122082543	0.05	444.06	1.02
	12	370	443364	0.04	426.08	0.87	120129022	0.05	436.95	0.85
	13	515	457632	0.05	439.79	1.17	120421639	0.05	438.02	1.18
	14	363	385366	0.04	370.34	0.98	124902244	0.05	454.31	0.80
	15	434	421638	0.04	405.20	1.07	104043685	0.04	378.44	1.15
	16	388	352343	0.04	338.61	1.15	98207768	0.04	357.22	1.09
	17	421	406240	0.04	390.40	1.08	94987271	0.04	345.50	1.22
	18	355	343227	0.03	329.85	1.08	90702639	0.03	329.92	1.08
	19	263	283813	0.03	272.75	0.96	61431566	0.02	223.45	1.18
	X	222	348647	0.03	335.06	0.66	171031299	0.06	622.10	0.36
		9580	**9968595**	**1.00**	**9580.00**	**1.00**	**2633776672**	**1.00**	**9580.00**	**1.00**

nondown-sampled	1	1058	848217	0.07	1063.29	1.00	195471971	0.07	1091.51	0.97
	2	949	885440	0.08	1109.95	0.85	182113224	0.07	1016.92	0.93
	3	908	619881	0.05	777.06	1.17	160039680	0.06	893.66	1.02
	4	847	733825	0.06	919.89	0.92	156508116	0.06	873.94	0.97
	5	1086	762355	0.06	955.66	1.14	151834684	0.06	847.84	1.28
	6	776	629796	0.05	789.49	0.98	149736546	0.06	836.13	0.93
	7	773	659722	0.06	827.00	0.93	145441459	0.06	812.14	0.95
	8	822	652477	0.06	817.92	1.00	129401213	0.05	722.58	1.14
	9	696	624655	0.05	783.04	0.89	124595110	0.05	695.74	1.00
	10	1121	613815	0.05	769.45	1.46	130694993	0.05	729.80	1.54
	11	722	716616	0.06	898.32	0.80	122082543	0.05	681.71	1.06
	12	551	521811	0.04	654.12	0.84	120129022	0.05	670.80	0.82
	13	777	532573	0.05	667.61	1.16	120421639	0.05	672.43	1.16
	14	627	482138	0.04	604.39	1.04	124902244	0.05	697.45	0.90
	15	627	488094	0.04	611.86	1.02	104043685	0.04	580.98	1.08
	16	578	406630	0.03	509.74	1.13	98207768	0.04	548.39	1.05
	17	637	480901	0.04	602.84	1.06	94987271	0.04	530.41	1.20
	18	525	395882	0.03	496.26	1.06	90702639	0.03	506.48	1.04
	19	389	328209	0.03	411.43	0.95	61431566	0.02	343.03	1.13
	X	238	349136	0.03	437.66	0.54	171031299	0.06	955.04	0.25
		14707	**11732173**	**1.00**	**14707.00**	**1.00**	**2633776672**	**1.00**	**14707.00**	**1.00**

Supplementary Citations

Benjamini Y., Hochberg Y., 1995 Controlling the false discovery rate: a practical and powerful approach to multiple testing. J R Stat Soc **57**: 289–300.

Li Y.-F., He W., Jha K. N., Klotz K., Kim Y.-H., Mandal A., Pulido S., Digilio L., Flickinger C. J., Herr J. C., 2007 FSCB, a novel protein kinase A-phosphorylated calcium-binding protein, is a CABYR-binding partner involved in late steps of fibrous sheath biogenesis. J Biol Chem **282**: 34104–34119.

Maekawa M., Ito C., Toyama Y., Suzuki-Toyota F., Kimura T., Nakano T., Toshimori K., 2004 Stage-specific expression of mouse germ cell-less-1 (mGCL-1), and multiple deformations during mgcl-1 deficient spermatogenesis leading to reduced fertility. Arch Histol Cytol **67**: 335–347.

Nguyen T. B., Manova K., Capodieci P., Lindon C., Bottega S., Wang X.-Y., Refik-Rogers J., Pines J., Wolgemuth D. J., Koff A., 2002 Characterization and expression of mammalian cyclin b3, a prepachytene meiotic cyclin. J Biol Chem **277**: 41960–41969.

Raymond C. S., Murphy M. W., O'Sullivan M. G., Bardwell V. J., Zarkower D., 2000 Dmrt1, a gene related to worm and fly sexual regulators, is required for mammalian testis differentiation. Genes Dev **14**: 2587–2595.